Colloquium: Beta-delayed fission of atomic nuclei

Andrei N. Andreyev*

Department of Physics, University of York, Heslington, York YO10 5DD, United Kingdom and Advanced Science Research Centre (ASRC), Japanese Atomic Energy Agency (JAEA), Tokai-mura, Japan

Mark Huyse and Piet Van Duppen

Instituut voor Kern-en Stralingsfysica, KU Leuven, University of Leuven, B-3001 Leuven, Belgium

(published 4 October 2013)

This Colloquium reviews the studies of exotic type of low-energy nuclear fission, the β-delayed fission (βDF). Emphasis is made on the new data from very neutron-deficient nuclei in the lead region, previously scarcely studied as far as fission is concerned. These data establish the new region of asymmetric fission in addition to the previously known one in the transuranium nuclei. New production and identification techniques, which emerged in the last two decades, such as the wider use of electromagnetic separators and the application of selective laser ionization to produce intense isotopically or even isomerically pure radioactive beams are highlighted. A critical analysis of presently available βDF data is presented and the importance of detailed quantitative βDF studies, which become possible now, is stressed, along with the recent theory efforts in the domain of low-energy fission.

DOI: 10.1103/RevModPhys.85.1541 PACS numbers: 24.75.+i, 25.85.−w, 29.38.−c

CONTENTS

I. INTRODUCTION

Nuclear fission, discovered in 1938 (Hahn and Strassmann, 1939), represents one of the most dramatic examples of a nuclear metamorphosis, whereby the nucleus splits preferentially into two smaller fragments releasing a large amount of energy. Historically, several distinctive types of fission were identified (Wagemans, 1991), such as particle-induced fission (Hahn and Strassmann, 1939), spontaneous fission (SF) (Petrzhak *et al.*, 1941), spontaneously fissioning isomers (Polikanov *et al.*, 1962), β-delayed fission (βDF, the subject of this review) (Kuznetsov *et al.*, 1966, 1967), electromagnetically induced (Coulomb excitation or Coulex) fission of radioactive nuclei at relativistic energies (Schmidt *et al.*, 2000; Schmidt, Benlliure, and Junghans, 2001), photofission (Csige *et al.*, 2013), and a surrogate type of fission (Escher *et al.*, 2012).

Fission is a unique tool to probe the nuclear potential-energy landscape and its evolution, as a complex function of elongation, mass asymmetry, spin, and excitation energy, from the single "compound nucleus" system over the top of the fission barrier and further to the scission point, culminating in the formation of fission fragments. This transition involves a subtle interplay of collective (macroscopic or mean field) and single-particle (microscopic) effects, such as shell effects and pairing, all of which considered both for the initial nucleus and for the final fission fragments and at large deformations. Fission enables the study of nuclear-structure effects in the heaviest nuclei (Armbruster, 1999) and has direct consequences on their creation in nuclear explosions (Wene and Johansson, 1974) and in the astrophysical *r* process (Panov *et al.*, 2005; Petermann *et al.*, 2012), which is terminated by fission, and on the abundance of medium-mass elements in the Universe through so-called "fission

*Andrei.Andreyev@york.ac.uk

recycling." Fission is also a very powerful mechanism to produce nuclei far from the stability line (Kugler, 2000). Apart from its importance for fundamental studies, fission has many practical applications, such as the generation of energy and the production of radioisotopes for science and medicine.

As a function of the excitation energy of the fissioning nucleus, the fission process is often broadly classified either as high-energy fission, in which the excitation energy strongly exceeds the fission-barrier height, or as low-energy fission. In contrast to high-energy fission, in which the microscopic effects are washed out, the interplay between macroscopic and microscopic effects in fission can be sensitively explored at low excitation energy. In particular, in SF from the ground state, the excitation energy is $E^* = 0$ MeV, while in SF from isomeric states or in thermal neutron-induced fission it does not exceed several MeV. However, being the ultimate tool for low-energy fission studies, SF is limited to heavy actinides and transactinides. For nonfissile nuclides, the photofission and surrogate fission techniques are especially valuable tools to probe the shape and height of fission barriers (Escher *et al.*, 2012; Csige *et al.*, 2013). Recently, by using Coulex-excited fission of relativistic radioactive beams, fission studies became available in new regions of the nuclidic chart with exotic N/Z ratios, earlier unexplored by low-energy fission (Schmidt *et al.*, 2000; Schmidt, Benlliure, and Junghans, 2001); see Fig. 1. In this case, the excitation energy is centered around $E^* \sim 11$ MeV. In terms of the excitation energy, βDF is intermediate between SF and Coulex-induced fission. Furthermore, presently, βDF allows one to access the most exotic cases of low-energy fission, not yet accessible by other techniques.

This Colloquium reviews the βDF data, collected since 1999, with an emphasis on the very neutron-deficient nuclei from the lead region, previously scarcely investigated as far as fission is concerned. By 1999 less than 20 βDF cases were known, and for most of them rather imprecise or even controversial data were reported. These studies, along with the conclusions drawn, were reviewed in 1992 (Hall and Hoffman, 1992) and in 1999 (Kuznetsov and Skobelev, 1999); a brief summary of the previous results is given in Sec. IV. Also the production and identification methods, which emerged in the last two decades, including the wider use of electromagnetic separators and the application of selective laser ionization (Fedosseev *et al.*, 2012), are addressed. A critical analysis of the presently available βDF data is presented and the need for detailed and quantitative βDF studies is emphasized. The recent theoretical efforts in the field of low-energy fission and future prospects for βDF studies are discussed in Secs. VI.C and VII, respectively. Table I summarizes all presently known βDF cases.

II. βDF: A TOOL TO STUDY LOW-ENERGY FISSION OF EXOTIC NUCLEI

Beta-delayed fission, discovered in 1965–1966 (Kuznetsov *et al.*, 1966, 1967; Skobelev and Skobelev, 1972), is a two-step nuclear decay process that couples β decay and fission. In this process, a parent nucleus first undergoes β decay, populating excited state(s) in the daughter nuclide. In the case of neutron-deficient nuclei, electron capture (EC) or β^+ decay is considered (referred to further as β^+/EC), while β^- decay happens on the neutron-rich side of the nuclidic chart. Figure 2 shows a simplified diagram of βDF for the case of neutron-deficient nuclei. If the excitation energy of these states E^* is comparable to or greater than the fission-barrier height B_f of the daughter nucleus ($E^* \sim B_f$), then fission may happen instantaneously in competition with other

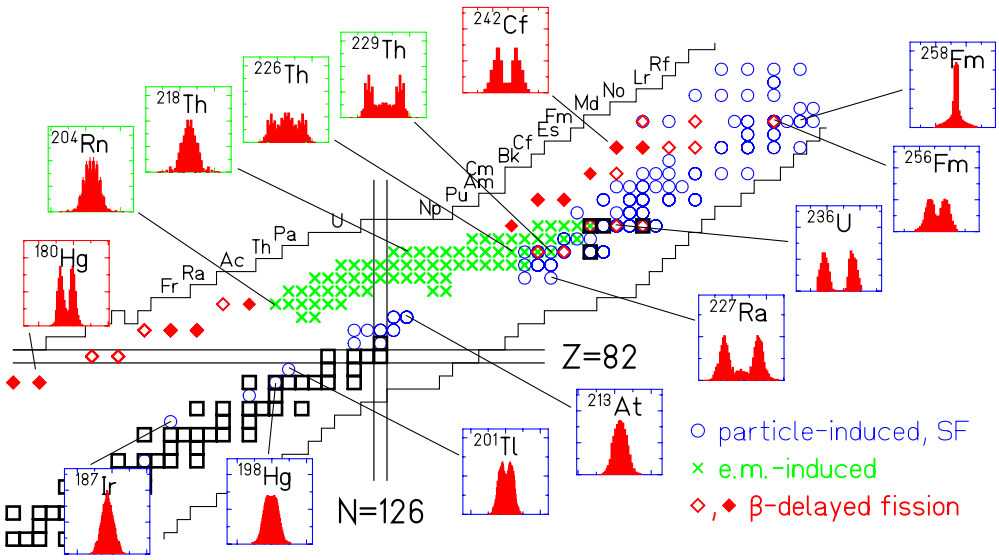

FIG. 1 (color online). The nuclei for which fission fragments mass or nuclear-charge distributions have been measured by low-energy fission. The distributions are shown for selected systems. Circles: distributions, measured in conventional particle-induced fission experiments and spontaneous fission. Crosses: nuclear-charge distributions, measured by Coulex excitation (Schmidt *et al.*, 2000; Schmidt, Benlliure, and Junghans, 2001). Diamonds: 26 known βDF cases; the fissioning daughter is indicated. Filled diamonds: 11 daughter nuclides for which mass distribution was measured, two of them (^{180}Hg and ^{242}Cf) are shown in the plot. References for βDF precursors are in Table I. Adapted from Schmidt and Jurado, 2012.

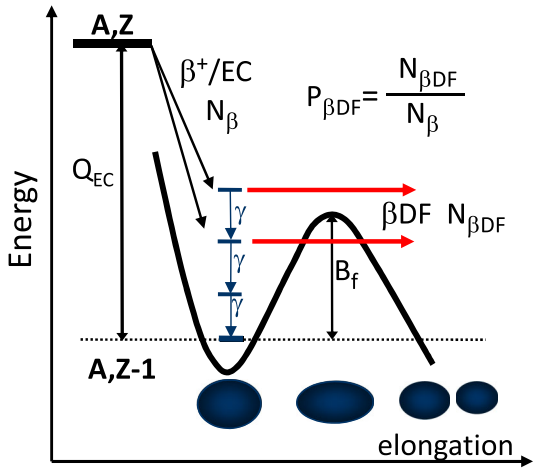

FIG. 2 (color online). Simplified diagram for the β^+/EC delayed fission in the neutron-deficient nuclei. Shown are the ground states of the parent (A, Z) and daughter $(A, Z-1)$ nuclei, and as a function of elongation, the potential energy of the daughter nucleus. The Q_{EC} value of the parent and fission barrier B_f of the daughter nuclei are indicated by vertical arrows. The βDF of excited states with $E^* \sim B_f$ in the daughter nucleus is shown by horizontal arrows.

decay modes, e.g., γ decay and/or particle emission (neutron, proton, or α), depending on which side of the β-stability valley the parent nucleus is situated. Therefore, the special feature of βDF is that fission proceeds from excited state(s) of the daughter nuclide, but the time behavior of the βDF events is determined by the half-life of the parent nucleus (as with, e.g., β-delayed γ and particle decays). As in most cases the β-decay half-lives are longer than tens of ms, it makes βDF more easily accessible for experimental studies.

Historically, the neutron-deficient nuclei in the uranium region became first available for βDF studies. Since the EC decay dominates over the β^+ decay in this region, the term EC-delayed fission (ECDF) was often used in the literature, while the term βDF was predominantly reserved for β^--delayed fission in the neutron-rich nuclei. However, since in the neutron-deficient lead region the β^+ decay can effectively compete with the EC decay, we use throughout this review the term βDF for both the neutron-rich and neutron-deficient nuclei.

A distinctive feature of βDF is its *low-energy* character. Previously, low-energy fission studies were limited to nuclei along the valley of stability from around thorium (Th) to rutherfordium (Rf) and above, mostly using SF and fission induced by thermal neutrons. A decade ago, Coulex-induced fission of radioactive beams (Schmidt *et al.*, 2000; Schmidt, Benlliure, and Junghans, 2001) extended low-energy fission studies to very neutron-deficient At-Rn isotopes, also revealing the predominantly symmetric fission in this region; see Fig. 1. The typical excitation energy in these studies is centered around $E^* \sim 11$ MeV, with tails to lower and higher energies. In βDF, the *maximum* excitation energy of the daughter nucleus is limited by the Q_{EC} (Q_{β^-} in case of neutron-rich nuclei) of the parent. The typical Q_{EC} (Q_{β^-}) values are in the range of 3–6 and 9–12 MeV for the known βDF nuclei in the transuranium and lead regions, respectively.

The importance of βDF is highlighted by its ability to provide low-energy fission data for very exotic nuclei which do not decay by SF and which are difficult to access by other techniques. As shown in Fig. 1, these nuclei lie very close to the border of known nuclei. Recently, extensive βDF studies in the very neutron-deficient nuclei between Tl and Fr have been performed, which constitute the core of this Colloquium. Fissioning nuclei in this region possess unusual neutron to proton ratios, e.g., $N/Z = 1.23$–1.25 for ^{178,180}Hg (see Sec. V.C.1) in contrast to a typical ratio of $N/Z = 1.55$–1.59 in the uranium region, where numerous SF and βDF cases are known. This allows one to investigate potential differences in the βDF process and its observables in the two regions, which differ in many nuclear-structure properties.

Moreover, the potential role of βDF for the *r*-process termination by fission (along with neutron-induced and spontaneous fission) is the subject of ongoing discussion (Panov *et al.*, 2005; Petermann *et al.*, 2012), also in view of its possible implications for the determination of the age of the Galaxy by the actinide geochronometers (Thielemann, Metzinger, and Klapdor, 1983; Meyer *et al.*, 1989).

A. Conditions for βDF occurrence and observation

Historically, the study of Berlovich and Novikov (1969) was the first to correctly interpret the fission, observed by Kuznetsov *et al.* (1966, 1967), as being due to βDF. Furthermore, based on the comparison of calculated Q_{EC,β^-} and B_f values, the existence of two extended regions of βDF was proposed, in the heavy neutron-deficient and in the neutron-rich nuclei. Two main conditions must be satisfied for βDF to occur in measurable quantities. First, the parent nucleus must possess a nonzero β-branching ratio ($b_\beta > 0$). Second, the Q_{EC,β^-} value of the parent nucleus must be comparable to or higher than the fission barrier of the daughter Q_{EC,β^-}(parent) $\sim B_f$(daughter). The latter explains the importance of β-strength function S_β(parent), which determines the population of excited states in the daughter nucleus, especially of those close to the top of the fission barrier; see, e.g., the recent review by Izosimov, Kalinnikov, and Solnyshkin (2011). Together with the subsequent competition between fission and deexcitation of the excited state(s), this determines the βDF probability; see, e.g., Habs *et al.* (1978), Klapdor *et al.* (1979), Staudt *et al.* (1990), Izosimov, Kalinnikov, and Solnyshkin (2011), and Veselský *et al.* (2012) and Sec. VI.B. We note that, below the top of the fission barrier, fission can occur only via the tunneling through the barrier, in competition with the gamma decay. For the states well below the top of the barrier, the gamma decay becomes the dominant decay mode.

Figure 3 shows the map of the neutron-deficient nuclei in the Hg-Md region, for which the calculated difference $Q_{\mathrm{EC}} - B_f$ is in the range between -3 and $+5$ MeV. We note that for the majority of βDF nuclei in the uranium and lead regions, discussed in our work, no experimental Q_{EC} and deduced B_f values exist. Therefore, to treat all nuclei on the same footing throughout the paper we use the calculated finite-range droplet model (FRDM) masses (Möller *et al.*, 1995) and calculated fission barriers from finite-range liquid droplet model (FRLDM) (Möller *et al.*, 2009). In the

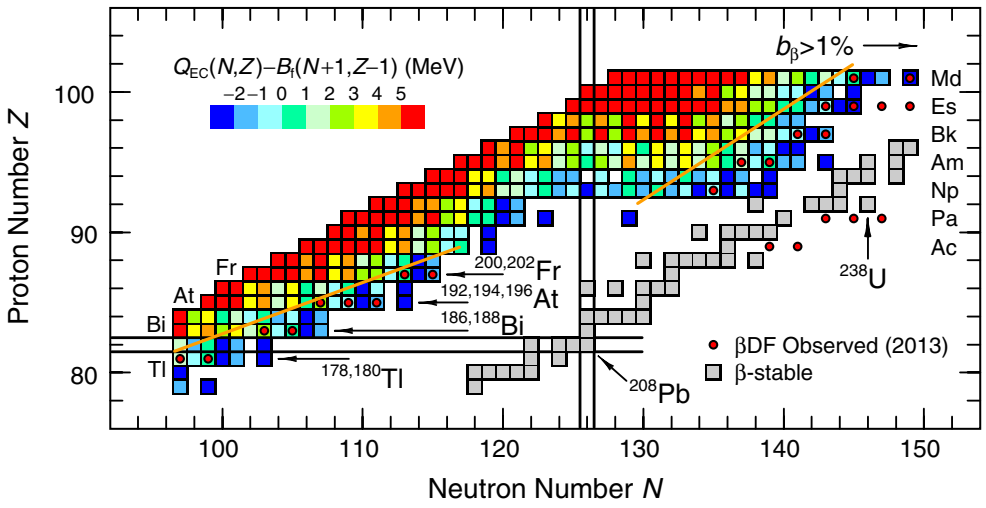

FIG. 3 (color online). Calculated Q_{EC}(parent) − B_f(daughter) difference for neutron-deficient Hg-Md nuclei within the framework of FRDM-FRLDM models. βDF is expected to be observable in the nuclei on the right-hand side of the sloped lines, which approximately delineate the region of nuclei with $b_\beta > 1\%$. The known βDF nuclei are marked by the circles. The references for data are in Table I. Adapted from Möller *et al.*, 2009.

following, we denote this model as FRDM-FRLDM. For comparison, we also use the Q_{EC} and B_f values from the Thomas-Fermi (TF) model (Myers and Świątecki, 1999). For the TF case, following the well-accepted procedure, the calculated microscopic shell corrections from FRDM were added to the calculated macroscopic TF fission barriers to derive the full TF fission-barrier heights, which can be directly compared to the FRLDM values.

We note, however, that at present it does not appear possible to establish which theoretical models provide a better agreement with fission barriers obtained by evaluating experimental data. Furthermore, the validity of the models may differ for different regions of nuclei, also as a function of the neutron number (Mamdouh *et al.*, 2001). As one example, the study reported by Möller *et al.* (2009) made a comprehensive comparison of the calculated (inner and outer) fission barriers with the available evaluated data for the thorium-einsteinium region. In most cases, the discrepancy between the calculated and evaluated values was less than 0.5 MeV, but in several cases discrepancies as large as 2 MeV were found, e.g., for the inner barriers of the thorium and protactinium isotopes. As many of the studied βDF nuclei are in this region of nuclei, one might expect that the FRDM-FRLDM approach should work quite satisfactorily for such nuclei, which explains our choice for this model. The use of the TF model will, however, give somewhat different quantitative results, as described next.

Based on the $Q_{EC} - B_f$ criterion alone, βDF could be observed for most of the nuclei in Fig. 3, apart from the β-stable ones. However, in the most neutron-deficient heavy isotopes α decay becomes the dominant decay mode. Therefore, the requirement of a nonzero β-branching ratio, set for a guidance as $b_\beta > 1\%$ in this plot, as achievable by modern experiments, strongly limits the number of nuclei where βDF can be observed to approximately 100 cases. All known neutron-deficient βDF nuclei were observed in the neutron-deficient transuranium and lead regions, separated by a region of Th-U isotopes with neutron numbers in the range of $N = 126$–130. The latter nuclei decay by fast α decays (half-lives in the sub-ms range) and presumably have very small β-branching ratios.

Table I shows that so far all known βDF emitters are odd-odd nuclei. To explain this point and to highlight common phenomena relevant to βDF, we analyze in Fig. 4 an example of βDF of At nuclei and compare the calculated Q_{EC} (At) and B_f (Po) values in the region of our interest for the FRDM-FRLDM and TF models. The extrapolated or experimental Q_{EC} (At) values (where known) from AME2012 (Audi *et al.*, 2012) are also plotted. However, the latter values should be considered with caution since in most of the lightest odd-odd astatine isotopes, e.g., in ^{192,194}At (Andreyev *et al.*, 2006, 2009), there is more than one long-lived nuclear state with unknown relative excitation energy and β-branching ratios. Furthermore, it is not always known which of them is the ground state and for which the experimental mass determination was quoted. This is a quite general issue in the odd-odd nuclei, which might influence the derivation of fission fragments mass distributions and probability values in βDF studies.

A few important features are evident in Fig. 4. First, the good agreement for the Q_{EC} (At) values between the two mass models is most probably because the Q_{EC} values are deduced as a difference of the calculated parent and daughter masses. Therefore, even if the two models give masses, systematically shifted by some value, this shift will largely cancel out in their difference.

Second, due to the odd-even staggering effect in masses, the Q_{EC} values of the odd-odd (thus, even-A) parent astatine isotopes are on average ∼1.5–2 MeV higher than for their odd-A neighbors. This is one of the main reasons why so far all observed βDF nuclei are odd-odd nuclei. Another reason is that after the β decay of an odd-odd isotope, an even-even daughter is produced, which is expected to fission more easily than an odd-A neighbor, produced after the β decay of an odd-A precursor. The very strong (several orders of magnitude) hindrance for SF of the odd-A and odd-odd nuclei in

TABLE I. Known βDF precursors. The half-life values are from either the original work or evaluated values from ENSDF (2013). $Q_{EC,\beta^-} - B_f$ differences are from the FRDM-FRLDM calculations. Eleven isotopes with reliably measured $P_{\beta DF}$ values (as evaluated by us, see Sec. VI.A) are marked in bold. They are used for evaluation of partial βDF half-lives in Fig. 12.

Isotope	$T_{1/2}$	$Q_{EC} - B_f$ (MeV)	Production,[a] separation, detection	$P_{\beta DF}$	Observables[b]	Reference
β^+/EC delayed fission in the neutron-deficient isotopes						
^{178}Tl	252(20) ms	1.82	SR, IS, WM	**$1.5(6)\times10^{-3}$**	*Z*, *A*, *T*, KE, TKE, MD, GF	Liberati *et al.* (2013)
^{180}Tl	1.09(1) s	0.63	SR, IS, WM	**$3.2(2)\times10^{-5}$**	*Z*, *A*, *T*, KE, TKE, MD, GF	Elseviers *et al.* (2013)
	$0.97^{+0.09}_{-0.08}$ s		FE, NS, MF	$\sim3\times10^{-(7\pm1)}$	*T*, *EXF*	Lazarev *et al.* (1987, 1992)
^{186m1,m2}Bi	9.8(4), 14.8(8) ms[c]	2.09	FE, RS, Si/Ge	7.6×10^{-2}[d]	*T*, *EXF*, KE, GF	Lane, Andreyev, and ? (2013)
^{188m1,m2}Bi	$\sim$0.3 s[e]	0.51	FE, NS, MF	3.4×10^{-4}[f,e]	*T*, *EXF*	Lazarev *et al.* (1992)
	265(10), 60(3) ms[c]		FE, RS, Si/Ge	$(0.16\text{–}0.48)\times10^{-2}$[g]	*T*, *EXF*, KE, GF	Lane, Andreyev, and ? (2013)
^{192m1,m2}At	88(6), 11.5(6) ms[c]	2.09	FE, RS, Si/Ge	$(7\text{–}35)\times10^{-2}$	*T*, *EXF*, KE, GF	Andreyev *et al.* (2013)
^{194m1,m2}At	310(8), 253(10) ms[c]	−0.04	FE, RS, Si/Ge	$\sim(0.8\text{–}1.6)\times10^{-2}$	*T*, *EXF*, KE, GF	Andreyev *et al.* (2013)
			SR, IS, WM		*Z*, *A*, *T*, KE, TKE, MD, GF	Andreyev *et al.* (2012)
^{196}At	$0.23^{+0.05}_{-0.03}$ s	−1.19	FE, NS, MF	8.8×10^{-4}[f]	*T*, *EXF*	Lazarev *et al.* (1992)
			SR, IS, WM		*Z*, *A*, *T*, KE, TKE, MD, GF	Andreyev *et al.* (2012)
^{200}Fr	49(4) ms[c]	0.82	SR, IS, WM		*Z*, *A*, *T*, KE, TKE, MD, GF	Andreyev *et al.* (2011)
^{202m1,m2}Fr	0.30(5), 0.29(5) s[c]	−1.17	SR, IS, WM		*Z*, *A*, *T*, KE, TKE, MD, GF	Andreyev *et al.* (2011)
^{228}Np	61.4(14) s	−0.87	FE, RC, MG	**$2.0(9)\times10^{-4}$**	*Z*, *T*, KE, TKE, MD, GF	Kreek *et al.* (1994a)
	60(5) s		FE, NS, MF		*T*, *EXF*	Kuznetsov *et al.* (1966)
^{232}Am	1.31(4) min	1.65	FE, RC, MG	**$6.9(10)\times10^{-4}$**	*Z*, *T*, KE, TKE, MD, GF	Hall *et al.* (1990a)
	55(7) s		FE, NS, Si	$(1.3^{+4}_{-0.8})\times10^{-2}$	T, KE	Habs *et al.* (1978)
	1.40(25) min		FE, NS, MF	6.96×10^{-2}	*T*, *EXF*	Kuznetsov *et al.* (1967)
^{234}Am	2.32(8) min	0.29	FE, RC, MG	**$6.6(18)\times10^{-5}$**	*Z*, *T*, KE, TKE, MD, GF	Hall *et al.* (1989b, 1990b)
	2.6(2) min		FE, NS, MF	$\sim6.95\times10^{-5}$	*T*, *EXF*	Kuznetsov *et al.* (1967)
^{238}Bk	144(5) s	−0.15	FE, RC, MG	**$4.8(20)\times10^{-4}$**	*Z*, *T*, KE, TKE, MD, GF	Kreek *et al.* (1994b)
^{240}Bk	4.2(8) min	−1.99	FE, NS, MF	**$(1.3^{+1.8}_{-0.7})\times10^{-5}$**	*T*	Galeriu (1983)
	5(2) min		FE, NS, MF	1×10^{-5}[h]	*T*	Gangrsky *et al.* (1980)
^{242}Es	11(3) s	−0.94	FE, RC, MG	**$0.6(2)\times10^{-2}$**	*Z*, *T*, KE, TKE, MD	Shaughnessy *et al.* (2000)
	5–25 s		FE, RS, Si	$1.4(8)\times10^{-2}$	*T*, KE	Hingmann *et al.* (1985)
	17.8(16) s		FE, RS, Si	$(1.3^{+1.2}_{-0.7})\times10^{-2}$	*T*, KE	Antalic *et al.* (2010)
^{244}Es	38(11) s	−2.24	FE, RC, MG	**$1.2(4)\times10^{-4}$**	*Z*, *T*, KE, TKE, MD	Shaughnessy *et al.* (2002)
			FE, NS, MF	1×10^{-4}[h]	*T*	Gangrsky *et al.* (1980)
^{246}Es	7.7(5) min	−3.47	FE, RC, MG	**$(3.7^{+8.5}_{-3.0})\times10^{-5}$**	*Z*, *T*, KE	Shaughnessy *et al.* (2001)
	8 min		FE, NS, MF	3×10^{-5}[h]	*T*	Gangrsky *et al.* (1980)
^{248}Es	23(3) min	−4.26	FE, RC, MG	**$3.5(18)\times10^{-6}$**	*Z*, *T*, KE	Shaughnessy *et al.* (2001)
			FE, NS, MF	3×10^{-7}[h]	*T*	Gangrsky *et al.* (1980)
^{246m1,m2}Md	0.9(2), 4.4(8) s	0.14	FE, RS, Si	$>1\times10^{-1}$	*T*, KE	Antalic *et al.* (2010)
	1.0(4) s[e]		FE, RS, Si	$\sim0.65\times10^{-1}$	*T*, KE	Ninov *et al.* (1996)
^{250}Md	52(6) s[c]	−2.64	FE, NS, MF	2×10^{-4}[h]	*T*	Gangrsky *et al.* (1980)
β^- delayed fission in the neutron-rich isotopes						
^{228}Ac	6.15(2) h[c]	−4.45	LLP, RC, MF/Ge	$5(2)\times10^{-12}$		Yanbing *et al.* (2006)
^{230}Ac	122(3) s[c]	−2.73	TR, RC, MF/Ge	$1.19(40)\times10^{-8}$		Shuanggui *et al.* (2001)
^{256m}Es	7.6 h[c]	−3.23	TR, RC, Si/Ge	2×10^{-5}	*T*, KE	Hall *et al.* (1989a)
^{234gs}Pa	6.70(5) h[c]	−2.55	NI, NS, MF	3×10^{-12}[i]	*T*	Gangrsky *et al.* (1978)
^{234m}Pa	1.159(11) min[c]		LLP, RC, MF	10^{-12}[i]	*T*	Gangrsky *et al.* (1978)
^{236}Pa	9.1(1) min[c]	−2.02	SR, RC, MF/Ge	$\sim10^{-9}$	*T*	Batist *et al.* (1977)
			FE/GI,NS,MF	10^{-9}[i]/3×10^{-10}[i]	*T*	Gangrsky *et al.* (1978)
^{238}Pa	2.3(1) min[c]	−2.14	NI, NS, MF	6×10^{-7}, 1×10^{-8}[i]	*T*	Gangrsky *et al.* (1978)
			NI, RC, MF	$<2.6\times10-8$		Baas-May, Kratz, and Trautmann (1985)

[a]Production: (SR) spallation, (FE) fusion evaporation, (TR) transfer, (GI/NI) γ/neutron induced, (LLP) long-lived precursors. Separation: (NS) no separation, (IS) ISOL, (RS) recoil separator, (RC) radiochemistry (*Z* confirmation). Detection: (MF) mica foil, (Si/Ge) silicon/germanium detectors, (MG) "merry-go-around", (WM) windmill system.
[b]Observables: *Z*, *A*, *T*, *EXF*: atomic number, mass, half-life, and excitation function of the precursor; KE, TKE, MD: kinetic energy, total kinetic energy, and mass distribution of fission fragments; GF: γ/X rays—fission fragment coincidences.
[c]Evaluated half-life value from ENSDF (2013).
[d]Uncertainty as "a factor of 5" due to the estimated b_β value and the presence of two isomers (Lane, Andreyev, and ?, 2013).
[e]Only one nuclear state was mentioned in the original work, presently two states are known.
[f]Deduced by Andreyev *et al.* (1993), with a relative uncertainty of a factor of 4.
[g]Uncertainty as "a factor of 4" due to the estimated b_β value and the presence of two isomers (Lane, Andreyev, and ?, 2013).
[h]Uncertainty is estimated as (+ 100%, −50%) (Gangrsky *et al.*, 1980).
[i]Uncertainty is reported as "an order of magnitude estimate" (Gangrsky *et al.*, 1978).

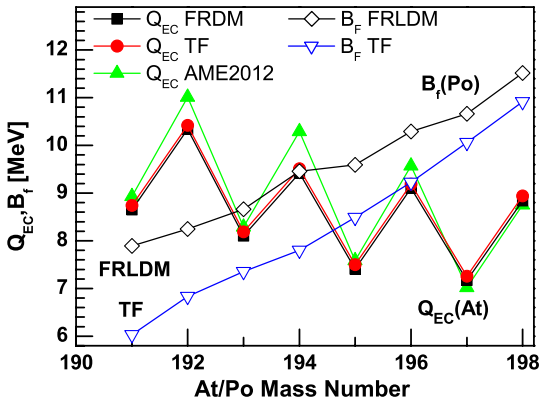

FIG. 4 (color online). Calculated Q_{EC} (At) values (filled symbols) for the parent At isotopes and calculated fission barriers B_f (Po) (open symbols) of the daughter Po isotopes according to the FRDM-FRLDM and TF models. The extrapolated or experimental Q_{EC} (At) values (where available) are from AME2012 (Audi *et al.*, 2012).

comparison with the even-even nuclides is a well-established experimental fact; see, e.g., Hoffman (1989). As the excitation energy of the fissioning daughter nucleus in βDF is relatively low, similar fission hindrance factors could also be expected for βDF; however, this is still an open question.

Another important feature of Fig. 4 is that both models predict a fast decrease of the calculated fission barriers, although the rate of decrease is different. Because of this, the respective calculated $Q_{\mathrm{EC}} - B_f$ values are quite different, e.g., 2.09 MeV (FRDM-FRLDM) and 3.59 MeV (TF) for ^{192}At. A similar effect occurs for many βDF cases in the lead region as discussed for ^{178}Tl (Liberati *et al.*, 2013) and ^{186,188}Bi (Lane, Andreyev, and ?, 2013). Clearly, the larger positive $Q_{\mathrm{EC}} - B_f$ values might open up the possibility of feeding states much higher above the fission barrier. Several studies explored the sensitivity of βDF probability values to the $Q_{\mathrm{EC}} - B_f$ differences to infer information on the fission-barrier height (Habs *et al.*, 1978; Klapdor *et al.*, 1979; Staudt *et al.*, 1990; Veselský *et al.*, 2012); thus to check the validity of different fission models far from the β-stability line, see Sec. VI.B.

Because of these energy arguments and considering a realistic experimental limit of 10^{-8}–10^{-7} for the βDF probability, as reliably achievable by the present-day experimental methods, the number of neutron-deficient βDF cases for which significant *quantitative* studies are presently possible is limited to ~40 cases.

The study (Berlovich and Novikov, 1969) also suggested the occurrence of βDF in the extended region of very neutron-rich nuclei with $Z \geq 86$ and neutron numbers in the range of 160–220. Since then, the role of βDF for the *r* process and its termination is the subject of active theoretical studies; see, e.g., Panov *et al.* (2005) and Petermann *et al.* (2012). However, the conclusions derived in such studies are quite sensitive to the assumptions used in the calculations. Experimentally, due to difficulties to reach these nuclei, very limited and often tentative or even controversial information is presently available, which will be critically assessed in this work.

One of the important questions to be addressed by βDF studies is whether the large difference in Q_{EC} and B_f values in the lead and transuranium regions plays any role. The density of states at the excitation energies in the vicinity of $E^* \sim Q_{\mathrm{EC}}$ in respective nuclei should be quite different, which could lead to different competition between γ-ray, fission, and particle decays of excited states in the daughter nucleus. Apart from energy considerations, the structure of the potential-energy surface on the way to fission differs dramatically in the two regions with a higher single-humped, but broader and somewhat flatter, fission barrier in the lead region and a lower, often two-humped, fission barrier in the uranium region; see Ichikawa *et al.* (2012) and Sec. VI.C.

B. βDF probability $P_{\beta\mathrm{DF}}$ and partial half-life $T_{1/2p,\beta\mathrm{DF}}$

Theoretically, the expression for $P_{\beta\mathrm{DF}}$ can be written in the form [see, e.g., Veselský *et al.* (2012)]

$$P_{\beta\mathrm{DF}} = \frac{N_{\beta\mathrm{DF}}}{N_\beta} = \frac{\int_0^{Q_\beta} F(Q_\beta - E) S_\beta(E) \Gamma_f(E)/\Gamma_{\mathrm{total}}(E) dE}{\int_0^{Q_\beta} F(Q_\beta - E) S_\beta(E) dE}, \quad (1)$$

where $F(Q_\beta - E)$ is the statistical Fermi function, $S_\beta(E)$ is the β-strength function, and $\Gamma_{\mathrm{total}}(E)$ is the total decay width of the excited state in the daughter nucleus, populated by β decay. In the most general case, such an excited state can decay via fission, or emission of a γ ray, proton, α particle or neutron, $\Gamma_{\mathrm{total}}(E) = \Gamma_f + \Gamma_\gamma + \Gamma_p + \Gamma_\alpha + \Gamma_n$. In the very neutron-deficient nuclei, typically only fission and γ-ray emission are considered as the dominant channels at excitation energies below the Q_{EC} value. On the neutron-rich side, the competition between the fission, γ, and neutron emission should be considered.

The experimental βDF probability $P_{\beta\mathrm{DF}}$ is defined as the ratio of the number of βDF decays $N_{\beta\mathrm{DF}}$ to the number of β decays of the parent nucleus N_β, $P_{\beta\mathrm{DF}} = N_{\beta\mathrm{DF}}/N_\beta$; see Fig. 2. The determination of $N_{\beta\mathrm{DF}}$ was not a trivial task in the earlier βDF experiments in which, after the production of the nuclei of interest, no pre-separation was used and mica foil detectors were often exploited for fission measurements. In such studies, the assignment was mostly based on the measured half-life of the fissioning activity, complemented in some cases with cross irradiations with different projectile-target combinations. Still, it is believed that, with some exceptions, the $N_{\beta\mathrm{DF}}$ value was reasonably well determined. In contrast to this, the number of β (especially β^+/EC) decays N_β is difficult to measure experimentally.

Therefore, in many earlier studies in the uranium region, in which β decay is often the dominant decay mode ($b_\beta \simeq 100\%$), N_β was estimated using the production cross section deduced from statistical model calculations. Such calculations were quite unreliable at that period and could potentially lead to large systematic errors as highlighted, for ^{180}Tl, for example, in Sec. V.C.1. To avoid this, some studies measured K x rays, originating from the EC decay, along with the K x rays, fission fragment coincidences, the latter uniquely proving the fact of βDF itself, as, e.g., in ^{228}Np (Kreek *et al.*, 1994a) and in ^{232,234}Am (Hall *et al.*, 1989b, 1990a, 1990b).

If the α-decay branch is not negligible, as, e.g., in the most neutron-deficient isotopes in the lead region, precise knowledge of the α- (or β-) branching ratio is needed, which often requires dedicated measurements. In their absence, the theoretical calculations of β-branching ratios are often exploited (Habs *et al.*, 1978; Andreyev *et al.*, 2013; Lane, Andreyev, and ?, 2013), which can lead to further uncertainties in the determination of $P_{\beta\mathrm{DF}}$ values.

The possible existence of two or more β-decaying isomeric states in the odd-odd parent further complicates βDF studies and can potentially lead to systematic errors in the determination of the βDF probability. This could especially be the case in many earlier studies, due to their insensitivity to the presence of isomers. Furthermore, in the uranium region, SF from the ground state of the daughter nucleus, which can be populated via three competing mechanisms: directly in the reaction, directly by the β decay, or via the γ-ray deexcitation from the excited state(s), must be considered. A recent βDF study of ^{246}Md (Antalic *et al.*, 2010) highlighted all these issues; see Sec. V.A.

By analogy with other decay modes, in this work we propose to introduce the partial βDF half-life

$$T_{1/2p,\beta\mathrm{DF}} = \frac{T_{1/2,\mathrm{tot}}}{b_\beta P_{\beta\mathrm{DF}}}$$

that corresponds to the inverse of the numerator of Eq. (1) and where $T_{1/2,\mathrm{tot}}$ is the total half-life of the nucleus. The partial βDF half-life does not only allow a more appropriate comparison with systematic trends, but can, in certain cases where the β-branching ratio is small and difficult to determine, still be obtained experimentally with acceptable accuracy.

For example, in the neutron-deficient isotopes in the lead region α decay is the dominant decay channel with α-branching ratios often being >90%. Furthermore, with the detection setups using silicon detectors, the ratio between the number of α and fission decays ($N_\alpha/N_{\beta\mathrm{DF}}$) can be accurately determined as both are measured in the same geometry. In this case the total half-life of the parent nucleus is close to the α-decay partial half-life ($T_{1/2,\mathrm{tot}} \simeq T_{1/2p,\alpha}$) and thus the partial experimental βDF half-life can be determined reliably as $T_{1/2p,\beta\mathrm{DF}} \simeq T_{1/2,\mathrm{tot}}(N_\alpha/N_{\beta\mathrm{DF}})$, while the experimental determination of the $P_{\beta\mathrm{DF}}$ value is more difficult.

The $T_{1/2p,\beta\mathrm{DF}}$ systematics and the use of the measured βDF probabilities to estimate the fission barrier are discussed in Sec. VI.B.

III. βDF PRODUCTION AND MEASUREMENT TECHNIQUES

This section summarizes production, separation, and detection techniques used specifically in βDF studies; see also column 4 of Table I.

A. Production methods

Four main production methods were exploited.

- Charged-particle induced reactions, typically fusion evaporation (FE) or transfer reactions (TR). The first βDF cases in ^{228}Np and ^{232,234}Am were identified in the FE reactions $^{10,11}\mathrm{B} + {}^{230}\mathrm{Th} \rightarrow {}^{232,234}\mathrm{Am}$ and $^{22}\mathrm{Ne} + {}^{209}\mathrm{Bi} \rightarrow {}^{228}\mathrm{Np}$ (Kuznetsov *et al.*, 1966, 1967). Several post-1999 βDF experiments also exploited FE reactions, e.g., the studies of ^{242,244,246,248}Es (Shaughnessy *et al.*, 2000, 2001, 2002; Antalic *et al.*, 2010), the identification of βDF in ^{192,194}At (Andreyev *et al.*, 2013) and in ^{186,188}Bi (Lane, Andreyev, and ?, 2013). Deep inelastic TR with heavy ions were exploited in, e.g., a βDF study of the neutron-rich ^{230}Ac (Shuanggui *et al.*, 2001).
- Spallation reactions (SR) with 1-GeV protons on a thick uranium target, followed by mass separation with an electromagnetic mass separator, were first used at the Investigation of Radioactive Isotopes on Synchrocyclotron (IRIS) (Gatchina) facility to search for βDF in very neutron-rich ^{228,230,232}Fr and ^{232}Ac (Mezilev *et al.*, 1990). No βDF was observed and the upper limits for βDF of these isotopes were estimated; see Table II. Recent experiments at the ISOLDE mass separator at CERN (Geneva) (Kugler, 2000) used the same method to identify βDF of ^{178,180}Tl (Andreyev *et al.*, 2010; Elseviers *et al.*, 2013; Liberati *et al.*, 2013), ^{194,196}At (Andreyev *et al.*, 2012), and ^{200,202}Fr (Andreyev *et al.*, 2011).
- Capture reactions induced by γ rays (GI) and neutrons (NI). By using neutron-induced reactions, the observation of βDF of the neutron-rich isotope ^{238}Pa was claimed by Gangrsky *et al.* (1978), which was, however, disputed in a later study (Baas-May, Kratz, and Trautmann, 1985), which used the same production method. βDF of ^{236}Pa, produced by using γ-rays induced reaction $^{238}\mathrm{U}(\gamma, np)^{236}\mathrm{Pa}$, was studied by Gangrsky *et al.* (1978).

TABLE II. βDF precursors for which only $P_{\beta\mathrm{DF}}$ limits were measured. For acronyms, see Table I.

Isotope	$T_{1/2}$	$Q_{\mathrm{EC}} - B_f$ (MeV)	Production, separation, detection	$P_{\beta\mathrm{DF}}$ Upper limit
^{242}Bk[a]	7.0(13) min[b]	−3.49	FE, NS, MF	$<3\times10^{-7}$
^{248}Md[a]	7(3) s[b]	−1.45	FE, NS, MF	$<5\times10^{-4}$
^{228}Fr[c]	38(1) s[b]	−3.33	SR, IS, Si/Ge	$<2\times10^{-7}$
^{230}Fr[c]	19.1(5) s[b]	−2.05	SR, IS, Si/Ge	$<3\times10^{-6}$
^{232}Fr[c]	5.5(6) s	−1.34	SR, IS, Si/Ge	$<7\times10^{-4}$[d]
^{232}Ac[c]	119(5) s	−1.75	SR, IS, Si	$<10^{-6}$

[a]Studied by Gangrsky *et al.* (1978).
[b]Evaluated half-life value from ENSDF (2013).
[c]Studied by Mezilev *et al.* (1990).
[d]Different limits for different β-γ transitions.

- Radiochemical separation from naturally occurring long-lived precursors (LLP). This method was used, e.g., to study βDF of the neutron-rich ^{234m}Pa (Gangrsky *et al.*, 1978), which was radiochemically separated from the products of the decay chain $^{238}\mathrm{U}\rightarrow^{\alpha}{}^{234}\mathrm{Th}\rightarrow^{\beta}{}^{234m}\mathrm{Pa}$. Similarly, βDF of the neutron-rich ^{228}Ac was studied after chemical separation from the products of the decay chain $^{232}\mathrm{Th}\rightarrow^{\alpha}{}^{228}\mathrm{Ra}\rightarrow^{\beta}{}^{228}\mathrm{Ac}$ (Yanbing *et al.*, 2006).

B. Separation and detection methods

Following the production, the βDF measurements can be broadly classified into three groups; see Table I: (1) no preseparation (NS) of produced radioactive nuclei before the detection of fission fragments, (2) radiochemical separation (RC), and (3) electromagnetic separation.

- No physical or chemical preseparation before the measurement of fission decays. The three main following methods were employed:
  (a) Direct viewing of the irradiated target by the fission detectors. In many earlier experiments mica fission (MF) foil detectors were used to directly view the thick target, which served as a recoil catcher. In some cases, this method allowed the measurement of the half-life of the fissioning activity, which was used for assignment to a specific nuclide. Often an extensive series of cross irradiations and excitation function measurements with different projectile-target combinations were performed to establish the βDF precursor. The insensitivity of MF to β particles prohibits the direct counting of the number of β decays, which is one of the ways to determine the βDF probability. Furthermore, no fission fragment energy information can be derived with MF and it is difficult to correctly account for the background from other fissioning products which could be simultaneously produced in the reaction and also from, e.g., SF of minute amounts of uranium and other neighboring nuclei.
  (b) Mechanical transport of activity to the detectors. In some cases, to avoid the high radiation background due to the target irradiation, the produced nuclei were allowed to recoil from the thin target and were transported some distance away from the irradiation zone. For example, in the βDF study of ^{232}Am (Habs *et al.*, 1978), the reaction products recoiling from the target were stopped in a carbon foil catcher downstream of the target. After irradiation the catcher was moved pneumatically in between two silicon detectors positioned 60 cm away from the target.
  (c) The He-jet technique. In this method, extensively applied by the Berkeley group, e.g., for the βDF studies of ^{242,244,246,248}Es (Shaughnessy *et al.*, 2000, 2001, 2002), the recoiling nuclei, typically produced in fusion-evaporation reactions, were captured in the He/KCl aerosol and quickly transported via a long and thin capillary to a detection system several tens of meters away from the irradiation zone. The activity was deposited on a sequential set of thin foils, surrounded by silicon and germanium detectors. In the literature, this system is often called a ''merry-go-around'' (MG) rotating wheel collection and detection system (Hoffman *et al.*, 1990). The combination of the thin source and silicon detectors allowed for the first time the measurement of the kinetic energies, total kinetic energies (TKE), and mass distribution for fission fragments. The measurements of x rays in coincidence with the fission fragments gave the first direct proof of the EC-delayed fission process in ^{232,234}Am (Hall *et al.*, 1989b, 1990a) and in ^{228}Np (Kreek *et al.*, 1994a). In some cases, e.g., βDF studies of ^{238}Bk (Kreek *et al.*, 1994b) and ^{228}Np (Kreek *et al.*, 1994a), the use of the He-jet technique was complemented by the subsequent radiochemical separation of the products (see below), extracted from the aerosol, to specifically select only the element of interest and produce a thin source. The above-mentioned MG system was used afterward.
- Radiochemical separation to provide the Z identification of the βDF precursor was used in many βDF studies and was reviewed by Hall and Hoffman (1992). In this method, the thick target (or the recoil catcher foil in the case of a thin target) is dissolved in an appropriate solvent, followed by radiochemical separation, aiming to extract a specific fraction containing only the element of interest and producing a thin source, which is further measured with fission detectors. The βDF studies of neutron-rich ^{228,230}Ac (Shuanggui *et al.*, 2001; Yanbing *et al.*, 2006) are the latest examples; see Sec. IV.
- Electromagnetic separation techniques rely on physical separation of the nuclei of interest from the products of different background reactions via two methods: in-flight recoil separation (RS) (Davids, 2003; Leino, 2003) or via the Isotope Separator On-Line (ISOL) method (Kugler, 2000). Both methods were used only occasionally in the pre-1999 studies.
  In-flight recoil separation provides very fast ($\sim \mu$s), but chemically unselective separation of the wanted products from the initial beam and some background products, e.g., prompt fission of the target nuclei. By using this method, the first identification of βDF of ^{242}Es (Hingmann *et al.*, 1985) and of ^{246}Md (Ninov *et al.*, 1996) has been performed at the velocity filter Separator for Heavy Ion Reaction Products (SHIP) [GSI (GSI Helmholtzzentrum für Schwerionenforschung)] (Münzenberg *et al.*, 1979). The βDF precursors were produced in fusion-evaporation reactions with heavy ions with a subsequent separation by SHIP. After the separation, the nuclei were implanted in a position sensitive silicon detector (PSSD), where their subsequent decays, including fission, were measured. The technique of time-position correlation of implanted nuclei with their subsequent decays strongly enhances the identification and assignment of observed decays to a specific isotope (Hofmann and Münzenberg, 2000). The RS technique becomes especially important in the case of βDF activities with half-lives in the tens of ms range, which is difficult to study by radiochemical, He-jet, or traditional ISOL methods. By using SHIP, new and so far the shortest-living, βDF activities were recently reported: ^{192,194}At [$T_{1/2}(^{192m1,m2}\mathrm{At}) \sim 12$ and 88 ms] (Andreyev *et al.*, 2013) and ^{186}Bi [$T_{1/2}(^{186m1,m2}\mathrm{Bi}) \sim 10$ and 15 ms] (Lane, Andreyev, and ?, 2013).

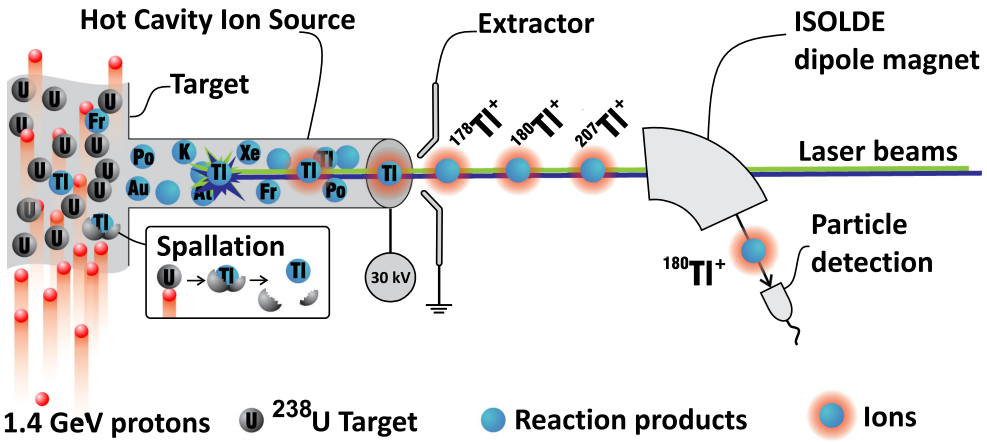

FIG. 5 (color online). Schematic view of the ISOLDE and RILIS operation as applied in the βDF studies of ^{180}Tl (Andreyev *et al.*, 2010; Elseviers *et al.*, 2013). The 1.4-GeV 2 μA proton beam impinges on the thick 50 g/cm^2 ^{238}U target, producing a variety of reaction products via the spallation, fragmentation, and fission reactions. The neutral reaction products diffuse toward the hot cavity where the thallium atoms are selectively ionized to a 1^+ charge state by two overlapping synchronized laser beams precisely tuned to provide thallium ionization in a two-color excitation and ionization scheme. The ionized thallium ions are extracted by the high-voltage potential of 30 kV, followed by the $A = 180$ mass separation with the ISOLDE dipole magnet. The mass-separated ^{180}Tl ions are finally implanted in the carbon foils of the windmill system, shown in Fig. 8, for subsequent measurements of their decays. Adapted from Rothe *et al.*, 2013.

The traditional application of the high-energy proton-induced spallation reactions and thick-target ISOL method, as used at, e.g., the ISOLDE mass separator (Kugler, 2000), allows the selection of nuclei with a specific mass number A, although usually no Z selection is obtained. The release of the ions from the ISOL target is much longer than the flight time in in-flight recoil separators and is also element dependent. So far, the shortest βDF isotopes measured by this techniques are ^{178}Tl [$T_{1/2} = 252(20)$ ms] (Liberati *et al.*, 2013) and ^{200}Fr ($T_{1/2} = 40$ ms) (Andreyev *et al.*, 2011).

Recently, the coupling of the resonance ionization laser ion source (RILIS) (Fedosseev *et al.*, 2012) to ISOLDE opened up new possibilities for βDF studies. The RILIS allows unique element-selective ionization of the element of interest, thus, Z identification. Figure 5 shows simplified operational principles of this technique as first used at ISOLDE for detailed βDF studies of ^{178,180}Tl (Andreyev *et al.*, 2010; Elseviers *et al.*, 2013; Liberati *et al.*, 2013); see Sec. V. The use of the laser ionization technique also allows unique *isomer* separation (Andreyev *et al.*, 2002), which is especially important for the odd-odd βDF precursors, many of which have more than one nuclear state capable of βDF; see Table I. An obvious drawback of the spallation-based ISOL method is that it can be applied only to elements lighter than the target uranium material; thus so far it was used only for βDF studies in the Tl-Fr region. In this respect, the recent development of the "In Gas Laser Ionization and Spectroscopy" (IGLIS) technique (Ferrer *et al.*, 2012), which can be applied employing reactions with heavy ions at ISOL systems or after an in-flight separator, could become crucial for detailed βDF studies in the transuranium region.

As summarized in Table I, most of the initial βDF studies in 1970–1980 used quite nonselective production and identification techniques, allowing only the fact of fission itself and the half-life of the fissioning activity to be measured. Over time, the application of radiochemical and electromagnetic separation, along with the developments in detection techniques, e.g., the wide use of silicon and germanium detectors, resulted in strong progress with βDF studies. Present-day experiments allow one to reliably access the much broader variety of observables; see column 6 of Table I.

IV. SUMMARY OF βDF DATA PRIOR TO 1999

A broad variety of different techniques was used in the earlier βDF investigations, with different degrees of selectivity in production and identification. This section highlights some of the common issues pertinent to the earlier studies, while we refer the interested reader to the reviews by Hall and Hoffman (1992) and Kuznetsov and Skobelev (1999) for a detailed survey of the pre-1999 results.

^{232}Am, being one of the first βDF nuclides discovered, provides a good example to demonstrate the relevant problems. The three $P_{\beta DF}$ values (see Table I) reported in the period of 1966–1990 disagree within a factor of 100. The discovery work by Kuznetsov *et al.* (1967) used mica detectors that directly viewed the irradiated target. Isotope assignment was performed based on the measured excitation function and half-life of the fissioning activity. However, to deduce the $P_{\beta DF}$ value, they estimated the production cross section of ^{232}Am with statistical model codes, which were quite unreliable at that time, especially for exotic nuclei. In the study by Habs *et al.* (1978), by using the movable catcher technique and silicon detectors, a $P_{\beta DF}$ value ~5 times lower than in the Dubna work was deduced, but to derive the N_β value, the α-branching ratio of ^{232}Am was estimated from systematics. In contrast to the two earlier studies, the work of Hall *et al.* (1990a) used the radiochemical separation of the americium fraction and the measurements of the daughter (after EC decay) plutonium K x rays to determine the N_β value. This method also relies on certain assumptions with

respect to internal conversion of plutonium γ-ray transitions, which was carefully analyzed by Hall *et al.* (1990a). Overall, they reported the most precise $P_{\beta DF}$ value, by a factor of 20–100 lower compared to Kuznetsov *et al.* (1967) and Habs *et al.* (1978).

On the other hand, it is interesting to note the good agreement between the $P_{\beta DF}$ values for ^{234}Am, measured by the same groups from Dubna (Kuznetsov *et al.*, 1967) and Berkeley (Hall *et al.*, 1989b, 1990b); see Table I. The same techniques as in the case of ^{232}Am were used, thus the reason for the difference by a factor of ~100 between respective measurements of ^{232}Am by Dubna and Berkeley is not clear at present, which was also highlighted by Hall *et al.* (1990a). It is important to remeasure the βDF of ^{232}Am in another experiment.

We also want to raise a concern related to the βDF data for the neutron-rich isotopes ^{234,236,238}Pa reported by Gangrsky *et al.* (1978). The measurements were performed with mica detectors without any preseparation. Based on a handful of observed fission events, some of the lowest βDF probability values in the range of 10^{-12}–10^{-8} were reported with an uncertainty quoted as an order of magnitude; see Table I. The βDF of ^{238}Pa was restudied by Baas-May, Kratz, and Trautmann (1985) with a radiochemical separation of the protactinium fraction from the irradiated sample, followed by measurements with the mica detectors. No fission events were observed, and they stated: "...From the absence of fission tracks an upper limit for the βDF probability of $P_{\beta DF}(^{238}\text{Pa}) \leq 2.6 \times 10^{-8}$ is obtained at 95% confidence level. This rules out positive evidence for this decay mode of ^{238}Pa reported elsewhere."

The case of ^{180}Tl, being the first βDF isotope discovered in the lead region (Lazarev *et al.*, 1987, 1992), is discussed in Sec. V.C.

Overall, for several nuclides in Table I, for which βDF was identified before 1999, only one single measurement exists. Furthermore, in contrast to traditional SF and particle-induced fission studies, for many βDF cases only the half-life and an estimate of βDF probability were reported, with no data on fission fragments energy-mass distributions or total kinetic energy.

V. POST-1999 RESULTS

The post-1999 period is characterized by a wider use of radiochemical and electromagnetic separation techniques. In several cases, the unique A and Z identification of the parent βDF isotopes became possible. The use of silicon detectors, which allows one to measure fission fragments' energies with a good precision, is another important improvement in comparison to earlier studies.

A. Neutron-deficient transuranium region

The Berkeley group made a substantial contribution to βDF studies in this region by remeasuring the properties of four isotopes ^{242,244,246,248}Es, produced in the fusion-evaporation reactions ^{233}U(^{14}N, $5n$)^{242}Es (Shaughnessy *et al.*, 2000), ^{237}Np(^{12}C, $5n$)^{244}Es (Shaughnessy *et al.*, 2002), ^{249}Cf(p, $4n$)^{246}Es (Shaughnessy *et al.*, 2001), and ^{249}Cf(p, $2n$)^{248}Es (Shaughnessy *et al.*, 2001). The He-jet technique and a merry-go-around detection system (Hoffman *et al.*, 1990) were used. Four pairs of coincident fission events were observed for ^{248}Es, one pair for ^{246}Es, 13 pairs for ^{244}Es, and 48 pairs for ^{242}Es. Despite the low number of βDF events observed for ^{242,244}Es the fission fragments' mass distributions for the respective daughter (after β^+/EC decay) isotopes ^{242,244}Cf were obtained; see Fig. 6 for ^{242}Cf. An asymmetric mass distribution for both cases was observed, which is characteristic for the low-energy fission of most nuclei in this region; see Fig. 1. We note that ^{250}Cf is the lightest californium isotope for which the fission mass distribution was measured by SF, thus the βDF studies extend the fission data to the more neutron-deficient region; see Fig. 1.

Within the experimental uncertainties, the three $P_{\beta DF}(^{242}\text{Es})$ values are consistent with each other, similar to the measurements for ^{244,246}Es made in Dubna (Gangrsky *et al.*, 1980) and Berkeley (Shaughnessy *et al.*, 2001, 2002); see Table I. However, a deviation by a factor of 10 was observed for ^{248}Es, being beyond the uncertainty values of the two studies (Gangrsky *et al.*, 1980; Shaughnessy *et al.*, 2001).

The βDF decay of the isotopes ^{246}Md and ^{242}Es was restudied at the velocity filter SHIP (Antalic *et al.*, 2010). After production in the fusion-evaporation reaction ^{209}Bi(^{40}Ar, $3n$)^{246}Md and separation with SHIP, the ^{246}Md nuclei were implanted into a PSSD, where subsequent particle and fission decays were measured. For ^{246}Md, the new state with a half-life of 4.4(8) s was identified in addition to the previously known state with a half-life of 0.9(2) s; see Fig. 7. This study highlighted one of the difficulties of the βDF experiments in the transuranium region, when the same fissioning even-even nucleus, in this case (isotope ^{246}Fm) is produced both as a daughter of an EC-decaying parent ^{246}Md and directly in the $p2n$ channel of the studied reaction, although presumably with a smaller cross section as estimated with the statistical model code (Antalic *et al.*, 2010). As ^{246}Fm has a non-negligible SF branch of 6.1%, a tedious decomposition of the observed fission events originating both from ECDF of ^{246}Md and from SF of ^{246}Fm had to be performed by Antalic *et al.* (2010). Thirty-seven fission decays were attributed to the βDF fission of the 4.4 s state

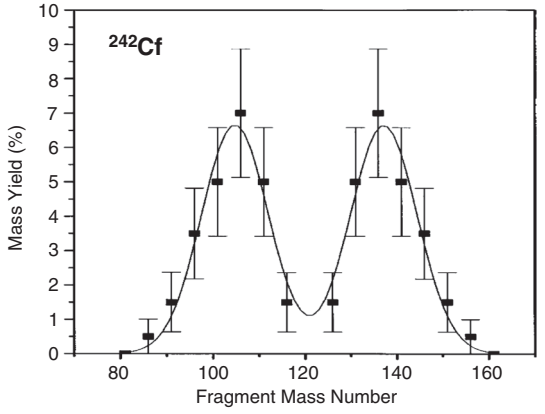

FIG. 6. Preneutron-emission mass-yield distribution for the βDF of ^{242}Es. The fissioning daughter nucleus is ^{242}Cf. From Shaughnessy *et al.*, 2000.

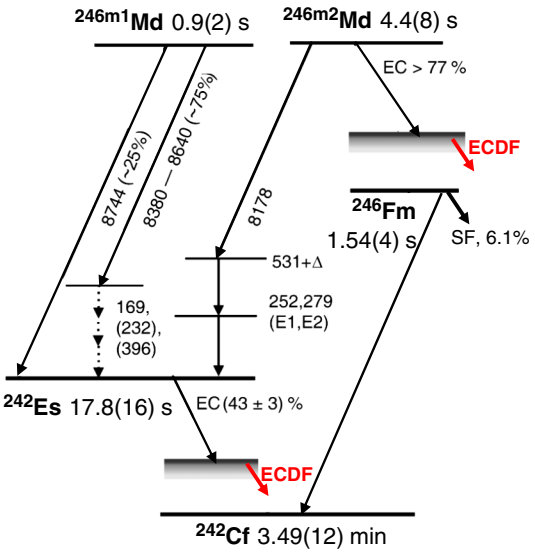

FIG. 7 (color online). Partial decay scheme of ^{246}Md modified from Antalic *et al.* (2010). The energies of the 4.4 and 0.9 s states are almost degenerate; however, no relative ordering could be given. They are denoted as $m1$ and $m2$. Shown are α-decay energies and EC-decay branches. The arrows marked by ECDF show schematically the fission of the excited state(s) in ^{246}Fm populated by EC decays of ^{246m2}Md (βDF of ^{246m2}Md) and fission of excited state(s) in ^{242}Cf, populated by the EC decay of ^{242}Es (βDF of ^{242}Es).

(^{246m2}Md), for which EC was deduced as the dominant decay mode ($b_{\mathrm{EC}} > 77\%$). Based on these data, they first deduced a value of $P_{\beta\mathrm{DF}}(^{246m2}\mathrm{Md}) = 1.3(3) \times 10^{-1}$, but after correction for a possible, but presumably small contribution due to the βDF of ^{246m1}Md, they finally quoted the lower limit estimate of $P_{\beta\mathrm{DF}}(^{246m2}\mathrm{Md}) > 1 \times 10^{-1}$. This lower limit is in broad agreement with the value of $\sim 0.65 \times 10^{-1}$ from an earlier study (Ninov *et al.*, 1996) also performed at SHIP. We note, however, that in Ninov *et al.* (1996) the observed βDF events were attributed to the shorter-lived 1.0(4) s state known in ^{246}Md at that time. This discrepancy is most probably due to much lower statistics (by at least a factor of 10) in the work of Ninov *et al.* (1996).

In the same study (Antalic *et al.*, 2010), the isotope ^{242}Es was produced after α decay of ^{246}Md; see Fig. 7. Based on the observation of three time-position correlated $\alpha(^{246}\mathrm{Md})$-fission events, they concluded that the fission events originated from the βDF of ^{242}Es and deduced a value of $P_{\beta\mathrm{DF}}(^{242}\mathrm{Es}) = (1.3^{+1.2}_{-0.7}) \times 10^{-2}$, consistent to previous studies.

B. βDF in neutron-rich nuclei

In contrast to the neutron-deficient nuclei, the progress with βDF studies of very neutron-rich nuclei is limited. This is due to large experimental difficulties to reach the most heavy neutron-rich nuclides for which βDF could have an observable branching ratio. To our knowledge, since the 1999 review, the βDF of only two neutron-rich isotopes ^{228,230}Ac was reported (Shuanggui *et al.*, 2001; Yanbing *et al.*, 2006), both investigated by the same group at the Heavy Ion Research Facility (HIRF) (Lanzhou, China).

To identify βDF of ^{230}Ac (the daughter of ^{230}Ra after β decay) the initial radioactive source was produced by 60 MeV/u ^{18}O irradiation of a thick 1.5 g/cm^2 ^{232}ThO$_2$ target. Afterward, the radium fraction was radiochemically separated from the mixture of the thorium target and reaction products, with 20 thin radium sources produced. The sources were exposed to the mica detectors, complemented with γ-ray measurements with a HPGe detector to check the isotopical content. The analysis of the γ-ray spectra showed that the radium source had dominant contributions from ^{230}Ra and its daughter ^{230}Ac and small amounts of $^{223-225,227}$Ra and their daughters after α decay. Two fission tracks were observed and attributed to βDF of ^{230}Ac. A value of $P_{\beta\mathrm{DF}}(^{230}\mathrm{Ac}) = 1.19(40) \times 10^{-8}$ was tentatively determined, but the reported uncertainty is clearly underestimated. This result should, however, be considered with caution as no mass separation was performed.

tβDF of ^{228}Ac (the daughter of ^{228}Ra after β decay) was studied after chemical separation of the radium fraction from the products of the decay chain of natural thorium $^{232}\mathrm{Th} \rightarrow^{\alpha} {}^{228}\mathrm{Ra}$ (Yanbing *et al.*, 2006). Twenty-two thin ^{228}Ra sources and five "blank" thorium sources were prepared and exposed to mica detectors for 720 days. The measurements with an HPGe γ-ray detector confirmed the purity of the radium source. In total 18 fission events were observed for the radium samples and one for the blank thorium samples. Therefore, the observed 17 fission events were attributed to βDF of ^{228}Ac, its βDF probability was deduced as $5(2) \times 10^{-12}$, being one of the lowest values reported for βDF.

C. Neutron-deficient lead region

βDF in the lead region was reported in 1987 (Lazarev *et al.*, 1987, 1992), by using fusion-evaporation reactions with heavy ions and mica detectors which directly viewed the irradiated target. Based on a large series of cross bombardments with different target-projectile combinations, three βDF nuclides were proposed, ^{180}Tl, ^{188}Bi, and ^{196}At; see Table I. The half-life and excitation functions of the fissioning activities were used for the βDF assignment. Only for ^{180}Tl, a βDF probability of $P_{\beta\mathrm{DF}} \sim 3 \times 10^{-(7\pm1)}$ could be deduced, approximately 2 orders of magnitude lower than expected from βDF systematics in the uranium region.

New experiments in the lead region, culminating in unambiguous confirmation and/or identification of βDF in the isotopes ^{178,180}Tl, ^{186,188}Bi, ^{192,194,196}At, and ^{200,202}Fr, were started in approximately 2008 and are summarized in this section. The electromagnetic separation techniques with ISOLDE (CERN) or with SHIP (GSI) were used.

1. ^{178,180}Tl at ISOLDE (CERN)

The βDF of ^{180}Tl was restudied at the ISOLDE mass separator (Andreyev *et al.*, 2010; Elseviers *et al.*, 2013); the production method is described in Fig. 5. After selective ionization, acceleration up to 30 keV, and mass separation, a pure ^{180}Tl beam of $\sim$150 atoms/s was analyzed by the windmill (WM) detection system shown in Fig. 8. The use of two silicon detectors in a compact geometry allowed both single α or fission decays and double-fold fission-fragment coincidences to be efficiently measured.

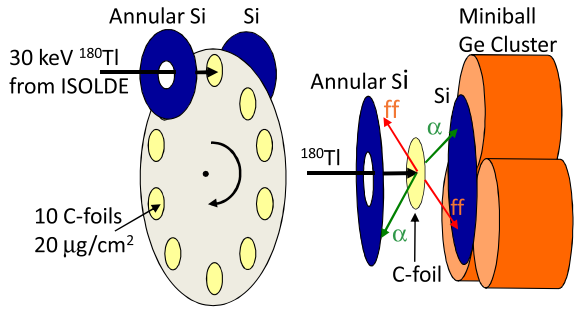

FIG. 8 (color online). Left: The windmill setup used in the experiments at ISOLDE to study βDF of ^{178,180}Tl, ^{194,196}At, and ^{200,202}Fr. Right: A zoom of the detector arrangement. The case of ^{180}Tl is shown as an example, with mass-separated ^{180}Tl ions being implanted through a hole in an annular silicon detector (300 μm thickness) into a thin carbon foil of 20 μg/cm^2 thickness. A second Si detector (300 μm thickness) is placed 3 mm behind the foil. A set of Ge detectors is used for γ- and K x-ray measurements in coincidence with particle decays. From Andreyev *et al.*, 2010.

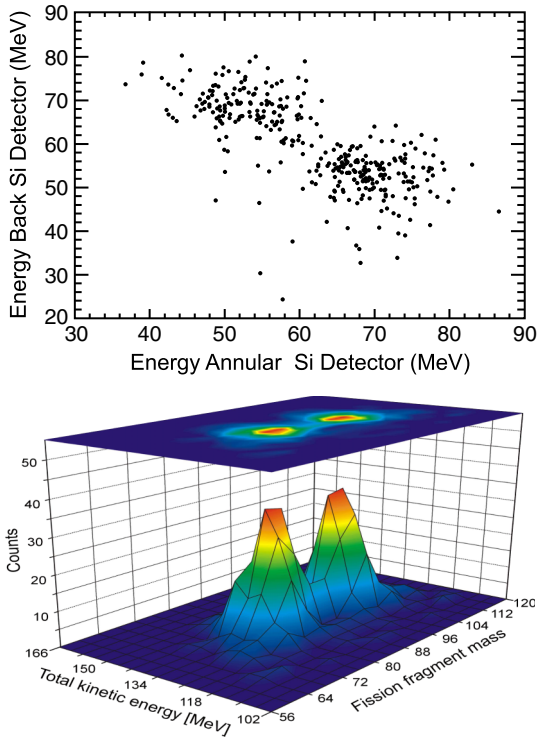

FIG. 9 (color online). Top: A coincidence energy spectrum for βDF of ^{180}Tl measured by two silicon detectors. The two-peaked structure originates because the two fission fragments have different energies, a direct result of the asymmetric mass distribution. Bottom: The derived fission-fragment distribution of the daughter isotope ^{180}Hg as a function of the fragment mass and the total kinetic energy; From Andreyev *et al.*, 2010 and Elseviers *et al.*, 2013.

The uniqueness of this technique is the unambiguous A and Z identification of the precursor, via the combination of the mass selection by ISOLDE and Z selection by the RILIS. Other advantages include a pointlike source, the implantation in a very thin foil whereby both fission fragments can be efficiently measured with little deterioration of their energies, and the proximity of germanium detectors for γ-ray spectroscopy. Simultaneous measurement of fission and α decays in the same detectors removes the systematic errors for branching ratio determination.

In an ~50-hour long experiment, 1111 singles and 356 coincidence fission events were observed and attributed to the βDF of ^{180}Tl; see Fig. 9. The mass distribution for fission fragments of ^{180}Hg is clearly asymmetric with the most abundantly produced fragments being ^{100}Ru and ^{80}Kr and their neighbors. However, a word of caution should be added here, as no direct Z identification was applied by authors and the deduced values are based on the assumption of the N/Z conservation in the fission process. No symmetric split in two semimagic ^{90}Zr nuclei was observed, and they claimed observation of a "new type of asymmetric fission in proton-rich nuclei," which differs from asymmetric fission in the transuranium region (Andreyev *et al.*, 2010; Ichikawa *et al.*, 2012).

Based on the energy balance (Andreyev *et al.*, 2010; Elseviers *et al.*, 2013), they claimed that only the evaporation of at most one neutron is energetically possible, which is due to both the relatively low excitation energy of the system and the high neutron separation energies of the neutron-deficient parent nucleus and fission fragments. Therefore, their conclusion on the most probable masses of fission fragments of ^{180}Hg is hardly sensitive to the assumption on the emission of neutrons. Most probably, the same inference will apply to other cases in the neutron-deficient lead region, discussed in this section. This situation is strongly different from that in the actinide region, where the account of the neutron multiplicity and its sawtooth behavior is a prerequisite to obtain the proper mass distribution (Balagna *et al.*, 1971).

The deduced βDF probability $P_{\beta\mathrm{DF}}(^{180}\mathrm{Tl}) = 3.2(2) \times 10^{-5}$ is approximately 100 times larger than the value reported by Lazarev *et al.* (1987, 1992). According to Andreyev *et al.* (2010) and Elseviers *et al.* (2013), the underestimated βDF probability in Dubna's study resulted from the strongly overestimated production cross section of ^{180}Tl (~ 0.1–1 mb), calculated with the statistical model code.

The βDF of ^{178}Tl was studied by the same group and method (Liberati *et al.*, 2013). The substantial yield drop (~ 0.1 atoms/s) compared to ^{180}Tl is due both to a decrease of the spallation cross section by moving toward the lighter isotope and its shorter half-life of ~250 ms. Despite the fact that only eight single fission events of ^{178}Hg (the daughter of ^{178}Tl after β decay) were observed, their energy distribution is clearly asymmetric and similar to that of βDF of ^{180}Tl; see Fig. 10. This means that the fission-fragment mass distribution for ^{178}Hg is also asymmetric. A value of $P_{\beta\mathrm{DF}}(^{178}\mathrm{Tl}) = 1.5(6) \times 10^{-3}$ was deduced, which is approximately 50 times larger than the respective value for ^{180}Tl.

The asymmetric mass distributions in the low-energy fission of ^{178,180}Hg establish a new region of the asymmetric mass split in fission, in addition to the previously known region of transuranium nuclei; see Fig. 1.

2. ^{200,202}Fr at ISOLDE (CERN)

The βDF of ^{200,202}Fr was identidied at ISOLDE (Andreyev *et al.*, 2011) by the same group and method as used for βDF of ^{178,180}Tl. No laser ion source was used as francium has a low ionization potential and is efficiently surface ionized in the hot cavity of the ion source, with negligible isobaric

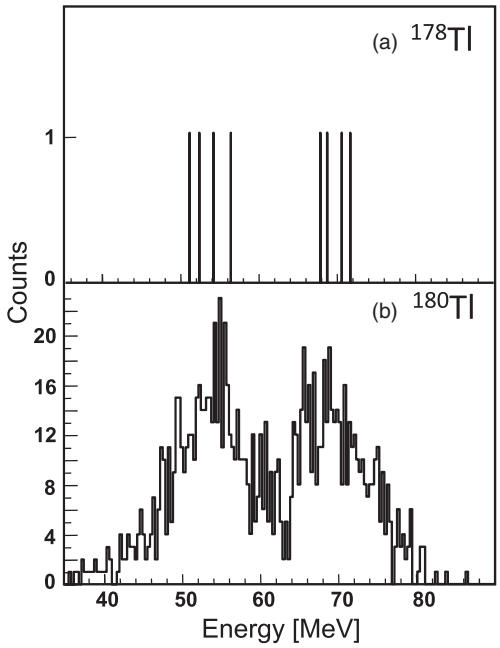

FIG. 10. Singles silicon energy spectrum for βDF of (a) ^{178}Tl and for βDF of (b) ^{180}Tl. From Liberati *et al.*, 2013.

contamination. 112 and 6 fission fragments were observed for ^{202}Fr and ^{200}Fr, respectively.

3. ^{192,194,196}At at SHIP (GSI)

βDF of ^{196}At was first reported in the study by Lazarev *et al.* (1992), which used the fusion-evaporation reaction ^{159}Tb(^{40}Ca, $3n$)^{196}At and mica detectors. 148 fission events were observed, but no βDF probability was reported. The later study by Andreyev *et al.* (1993), using the same reaction, derived a value of $P_{\beta\mathrm{DF}}(^{196}\mathrm{At}) = 8.8 \times 10^{-4}$, with a relative uncertainty of a factor of 4; see Table I. This was done by comparing the production cross section of ^{196}At from Andreyev *et al.* (1993) with the fission cross section, reported in Lazarev *et al.* (1992) and using a theoretical b_β value for ^{196}At.

βDF of ^{192,194}At was identified (Andreyev *et al.*, 2013) in the experiments at SHIP, by using fusion-evaporation reactions ^{144}Sm(^{51}V, $3n$)^{192}At and ^{141}Pr(^{56}Fe, $3n$)^{194}At. The same method, as described earlier for ^{246}Md, was used, with separated nuclei implanted in a PSSD.

Figure 11(a) shows the energy spectrum of all events registered in the PSSD in the βDF study of ^{194}At, while Fig. 11(b) shows the events registered only during the 15 ms "beam off" time interval, thus only *decay* events can be present in the spectrum. The 66 high-energy events in this spectrum were attributed to βDF of ^{194}At (^{194}Po being the fissioning daughter). Because of the presence of two isomeric states in ^{194}At with quite similar half-lives (see Table I) and due to yet unknown β-branching ratios for both isomers, only an estimate of the βDF probability was provided by the authors. As stated in Andreyev *et al.* (2013): "... βDF probability for ^{194}At should be in the percents range, which would be approximately an order of magnitude larger than the value of $P_{\beta\mathrm{DF}}(^{196}\mathrm{At}) = 8.8 \times 10^{-4}$, albeit with a relative uncertainty of factor 4, deduced in Andreyev *et al.* (1993)."

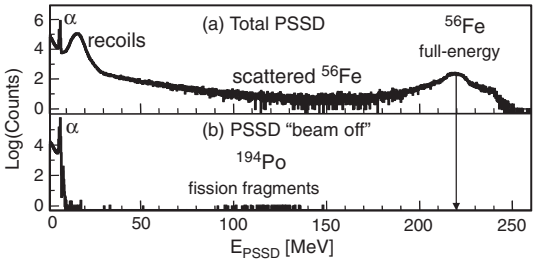

FIG. 11. (a) Total energy spectrum in the PSSD in the reaction ^{141}Pr(^{56}Fe, $3n$)^{194}At at the beam energy of $E(^{56}\mathrm{Fe}) = 259(1)$ MeV in front of the target. (b) The same as (a), but within 15 ms of the "beam off" interval, showing the 66 fission events of ^{194}Po. Adapted from Andreyev *et al.*, 2013.

By using the same technique, 24 βDF events were observed for ^{192}At (Andreyev *et al.*, 2013). Similar to the ^{194}At case, due to the presence of two isomeric states in ^{192}At, only an estimate of βDF probability was provided by Andreyev *et al.* (2013), who stated that "for two isomers in ^{192}At, values in the range of (7–35)% could be estimated, being the largest ever reported so far for βDF."

For completeness, we note that a more detailed βDF study of ^{194,196}At (Andreyev *et al.*, 2012) was recently performed at the mass separator ISOLDE. This work benefits from the recent development of an efficient ionization scheme for astatine (Rothe *et al.*, 2013).

4. ^{186,188}Bi at SHIP (GSI)

βDF in bismuth isotopes was first observed for ^{188}Bi by using a series of fusion-evaporation reactions and mica detectors (Lazarev *et al.*, 1992). No $P_{\beta\mathrm{DF}}$ value was reported, but similar to ^{196}At, a value of $P_{\beta\mathrm{DF}}(^{188}\mathrm{Bi}) = 3.4 \times 10^{-4}$ with a relative uncertainty of a factor of 4 was estimated by Andreyev *et al.* (1993).

In the experiments at SHIP, the same group which also studied ^{192,194}At, confirmed the occurrence of βDF for ^{188}Bi and identified βDF for ^{186}Bi (Lane, Andreyev, and ?, 2013). Four βDF events of ^{188}Bi (fission of daughter ^{188}Pb) were identified in the reaction ^{142}Nb(^{50}Cr, $p3n$)^{188}Bi. Three βDF events were assigned to ^{186}Bi (fission of daughter ^{186}Pb) which was studied in the reaction ^{144}Sm(^{46}Ti, $p3n$)^{186}Bi. The determination of $P_{\beta\mathrm{DF}}(^{186,188}\mathrm{Bi})$ values was hampered by the presence of two isomeric states in both nuclei, with yet unknown and small (in the percents range) β-branching ratios. As stated by Lane, Andreyev, and ? (2013), "an estimate of $P_{\beta\mathrm{DF}}(^{186m1,m2}\mathrm{Bi}) = 7.6 \times 10^{-2}$ was derived for both isomers, with an uncertainty of a factor of 5." For ^{188m1,m2}Bi, values in the range of $\sim(0.16\text{–}0.48) \times 10^{-2}$, with an uncertainty of a factor of 4, were proposed.

To summarize this section, only for ^{178,180}Tl are the rather precise βDF probability values presently available in the neutron-deficient lead region. On the other hand, a clear trend for a strong increase of $P_{\beta\mathrm{DF}}$ values is observed by moving toward the most neutron-deficient isotopes in each isotopic chain of Tl, Bi, and At. The values in the vicinity of tens of percent are estimated for the very neutron-deficient ^{186}Bi and ^{192}At, being some of the largest observed so far for βDF.

VI. DISCUSSION

The presently available experimental βDF data are summarized in columns 5 and 6 of Table I, the most important of them being the βDF probability and energy-mass characteristics for fission fragments. This section reviews the relevant systematics and recent theoretical efforts for βDF and low-energy fission in general.

A. Systematics of βDF partial half-lives

We propose to divide all known βDF precursors in Table I into two groups: one where the $P_{\beta\mathrm{DF}}$ value is solely based on measured quantities and one where theoretical estimations were needed. The first group consists of 11 isotopes: ^{178,180}Tl, ^{228}Np, ^{232,234}Am, ^{238,240}Bk, and ^{242,244,246,248}Es (marked in bold in Table I). In most cases, to determine N_β, the experimental β-branching ratio was used, along with the measured production cross section. Some of the $P_{\beta\mathrm{DF}}$ values were measured by at least two different teams with comparable results. We explicitly mention that we selected $P_{\beta\mathrm{DF}}(^{232}\mathrm{Am})$ from the Berkeley study (Hall *et al.*, 1990a) for this group as the two earlier measurements (Kuznetsov *et al.*, 1967; Habs *et al.*, 1978) belong to the second group.

For nuclei in the second group, to determinate the $P_{\beta\mathrm{DF}}$ value typically the calculations of the production cross section of the precursor, as, e.g., for ^{180}Tl (Lazarev *et al.*, 1992), and/or of the β-branching ratio, as, e.g., for ^{186,188}Bi, were used. In some of the experiments, only a small number of events was obtained, and such cases should be considered with caution, especially if no separation was used. The possible presence of isomeric states in the βDF precursor must be carefully considered in several cases, e.g., in ^{186,188}Bi, ^{192,194}At, ^{202}Fr, and ^{246}Md.

Following Sec. II.B, to generalize the discussion and to open up the possibility to include future βDF cases where the β-branching ratio is low (e.g., $b_\beta < 1\%$) and difficult to determine, we use βDF partial half-lives. Figures 12(a) and 12(b) show the $T_{1/2p,\beta\mathrm{DF}}$ values for the 11 nuclides from the first group as a function of the Q_{EC} value for the FRDM-FRLDM and TF models. The plots look alike, which is a consequence of the very similar Q_{EC} values given by both models. A striking linear dependence for the nine cases in the uranium region is evident, with all the data closely grouped alone the line. This fact was first stressed by the Berkeley team (Shaughnessy *et al.*, 2002) in the case of $P_{\beta\mathrm{DF}}(^{244}\mathrm{Es})$. Furthermore, the Tl data lie on a line with a similar slope, but the line is shifted due to much higher Q_{EC} (Tl) values. However, following the discussion of the βDF mechanism in Fig. 2, it could be expected that the βDF partial half-life should depend on the $Q_{\mathrm{EC}} - B_f$ difference. Therefore, Figs. 12(c) and 12(d) show the $T_{1/2p,\beta\mathrm{DF}}$ as a function of the $Q_{\mathrm{EC}} - B_f$ values. A very different behavior in the two models is apparent. Because of different B_f values, calculated by the two models, only 3 out of 11 cases should be considered as sub-barrier fission ($Q_{\mathrm{EC}} - B_f < 0$) in the TF model, in contrast to seven cases in the framework of FRDM-FRLDM. Interestingly, despite the fact that all four ^{242,224,246,248}Es isotopes are sub-barrier in the FRDM-FRLDM approach and only ^{246,248}Es are sub-barrier in the TF model, the linear dependence for all Es isotopes as a function of the $Q_{\mathrm{EC}} - B_f$ value is conserved in both models. Finally, in the TF model [Fig. 12(d)], all 11 values appear to follow the same linear dependence, although not as tightly as in Fig. 12(b). In contrast to this, different isotopic chains in Fig. 12(c) fall on different, but nearly parallel lines, with no obvious systematical dependence on the atomic number. The slopes of the lines seem to be comparable to that of the linear trend in the TF model. Presently, no clear explanations can be given for all these observations.

To shed more light on these observations, reliable $T_{1/2p,\beta\mathrm{DF}}$ data for even more neutron-deficient βDF isotopes in the uranium region, having higher Q_{EC} and $Q_{\mathrm{EC}} - B_f$ values, are needed. In the lead region, data are required for the Bi, At, and Fr isotopic chains. Taken together, it will allow a systematical comparison of βDF properties in the two regions, with the aim to disentangle the influence of the Q_{EC} and B_f values on the βDF probability. The next section explores the

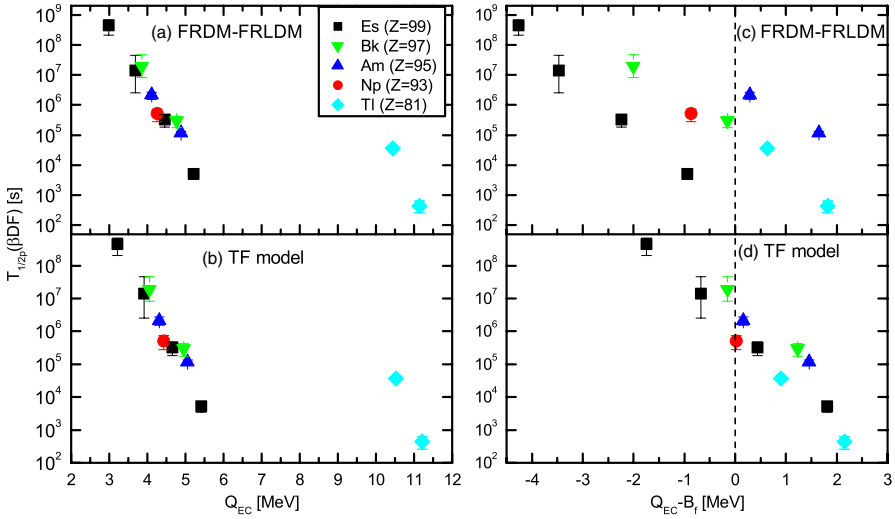

FIG. 12 (color online). Partial βDF half-lives (on a logarithm scale) for ^{178,180}Tl, ^{228}Np, ^{232,234}Am, ^{238,240}Bk, and ^{242,244,246,248}Es as a function of the Q_{EC} value for (a) FRDM-FRLDM and (b) TF models. (c) and (d) The same, but as a function of the $Q_{\mathrm{EC}} - B_f$ value.

link between $P_{\beta\mathrm{DF}}$ (or $T_{1/2p,\beta\mathrm{DF}}$) systematics and the fission barriers.

B. Estimation of fission barriers from $P_{\beta\mathrm{DF}}$ values

The use of Eq. (1), with specific assumptions on its different ingredients, allows one to estimate the fission barrier B_f from the experimental $P_{\beta\mathrm{DF}}$ values. The application of this, admittedly model-dependent, approach for the transuranium region was discussed in several earlier studies, see, e.g., Habs *et al.* (1978), Gangrsky *et al.* (1980), and Galeriu (1983) and was thoroughly reviewed by Hall and Hoffman (1992), Kuznetsov and Skobelev (1999), and Izosimov, Kalinnikov, and Solnyshkin (2011).

In the lead region, this approach was used to estimate the fission barriers of ^{188}Pb and ^{196}Po (Andreyev *et al.*, 1993). The deduced fission barriers were lower than the values calculated by several theoretical approaches. We, however, note that the $P_{\beta\mathrm{DF}}(^{188}\mathrm{Bi})$ value from Andreyev *et al.* (1993) was used, without taking into account the presence of two isomeric states in ^{188}Bi. The study by Staudt *et al.* (1990) made the $B_f(^{180}\mathrm{Hg})$ estimation by using the strongly underestimated $P_{\beta\mathrm{DF}}(^{180}\mathrm{Tl})$ value from Lazarev *et al.* (1987, 1992).

The recent comprehensive study by Veselský *et al.* (2012) extracted the fission barriers of ^{178,180}Hg from the βDF probabilities for ^{178,180}Tl reported by Elseviers *et al.* (2013) and Liberati *et al.* (2013). Four alternative β-decay strength functions were used, including the so-called "flat" strength function and also strength functions which had a clear resonance structure. Furthermore, four variants of a statistical model of deexcitation of the daughter nucleus were used which allowed one to thoroughly investigate the sensitivity of the obtained results on the choice of parameters. No strong sensitivity to the choice of the β-strength function was noted. This is a somewhat surprising result, as one expected to see the influence of the resonance structure of the β-strength function, which is typical in β decay as shown in the comprehensive review work by Izosimov, Kalinnikov, and Solnyshkin (2011). Furthermore, the study of Izosimov, Kalinnikov, and Solnyshkin (2011) stressed the need of taking into account the nonstatistical effects of the β-strength function in such calculations, at least in the actinides region. The experimental determination of the strength function could help to avoid possible ambiguities related to the choice of some of the parameters. Depending on the choice of the statistical model, the deduced fission-barrier heights appeared to be 10%–40% smaller than the theoretical estimates from several approaches, including the ones from the FRLDM (Möller *et al.*, 2009) used for the this study.

Thus, it appears that the fission barriers deduced from the βDF studies in the lead region confirm an earlier inference on the reduced fission barriers obtained from data on cross sections of heavy ion reactions leading to the same nuclei; see Andreyev *et al.* (2005) and references therein.

C. Theoretical studies of the fission mass distributions of mercury isotopes and low-energy fission

Other important observables which become systematically accessible via the βDF studies are the energy and mass distributions of the fission fragments for extremely neutron-deficient nuclides. The recent βDF studies in the lead region triggered a series of calculations by several theory groups, which are reviewed in this section.

In the βDF study of ^{180}Tl (Andreyev *et al.*, 2010), the five-dimensional (5D) macroscopic-microscopic model (Möller *et al.*, 2001) was applied to explain the observed asymmetric mass split of the fission fragments of ^{180}Hg. In a follow-up study (Ichikawa *et al.*, 2012), the two-dimensional potential-energy surfaces (PES) for ^{180}Hg and ^{236}U, extracted from the 5D model, were discussed to analyze the differences in the nature of asymmetric fission for proton-rich nuclei in the lead region compared to the more familiar actinide region; see Fig. 13.

The PES for ^{236}U shows features common to many actinide nuclei with $226 \leq A \leq 256$, such as a deformed ground state, a relatively low two- or three-peaked fission barrier, and most

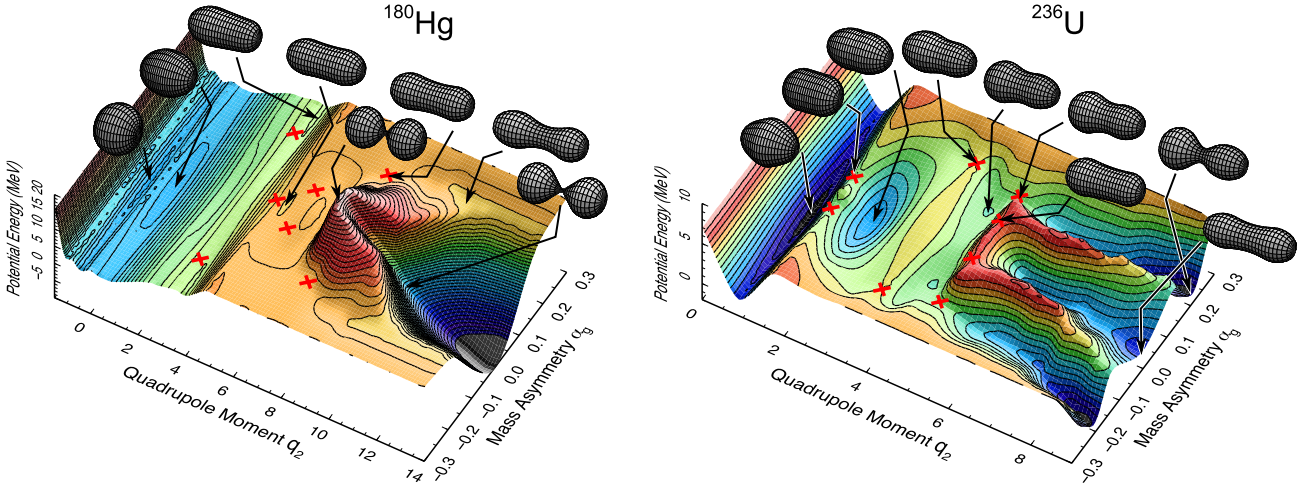

FIG. 13 (color online). Calculated PES surfaces for ^{180}Hg and ^{236}U as a function of the dimensionless quadrupole moment and the mass asymmetry. The shapes of the nuclei at several key locations as they proceed to fission are drawn, connected to the points on the surface by arrows. Adapted from Ichikawa *et al.*, 2012.

prominently, well-separated symmetric ($\alpha_g = 0$) and asymmetric ($\alpha_g \sim 0.2$) valleys. The higher symmetric saddle reduces the probability of entering the symmetric valley by requiring barrier penetration for systems with near-threshold energies.

For ^{180}Hg the PES is very different, with only a single pronounced symmetric valley corresponding to separated semimagic ^{90}Zr nuclei, and no deep asymmetric valley extending to scission. The dominant symmetric valley is inaccessible due to the high barrier along the symmetric path from the ground state. The symmetric valley remains separated from a shallow asymmetric valley by a high ridge in the potential. An important finding of Ichikawa *et al.* (2012) is that only isotopes with $180 \leq A(\mathrm{Hg}) \leq 190$ have this feature of a shallow asymmetric valley extending from the saddle point to fairly elongated shapes with small necks. One may speculate, as Andreyev *et al.* (2010), that the relatively small neck radius where the asymmetric valley vanishes prevents complete mass transfer before scission.

As a follow-up development, the fission of even-A isotopes of Hg was analyzed (Möller, Randrup, and Sierk, 2012) with a Brownian shape motion model combined with the Metropolis algorithm (Randrup and Möller, 2011). The model needs only a PES and a level-density approximation which relates thermal excitation energy to nuclear temperature T. It also predicts mass-asymmetric distributions at low excitation energy for $178 \leq A(\mathrm{Hg}) \leq 188$.

The self-consistent nuclear density functional theory employing Skyrme SKM* and Gogny D1S energy density functionals was used by Warda, Staszczak, and Nazarewicz (2012) to study the fission of ^{180}Hg and ^{198}Hg. In both models the PES was determined in a multidimensional space of collective coordinates spanned by quadrupole and octupole moments for describing elongation and reflection asymmetry of the system, respectively. The asymmetric fission valleys, well separated from fusion valleys associated with nearly spherical fragments, were found in both cases. Symmetric shapes of a nucleus are predicted on the fission path for small deformations whereas elongated configurations favor octupole deformed distributions. Reflection asymmetry obtained at the scission point lead to the mass asymmetry of the fission fragments. The most probable split predicted in both models is consistent with the experimentally observed ^{100}Ru/^{80}Kr.

Two further approaches were inspired by the earlier scission-point model (Wilkins, Steinberg, and Chasman, 1976). In the work of Andreev, Adamian, and Antonenko (2012), by using what was called the ''improved scission-point'' model, the mass, charge, as well as the kinetic energy distributions are calculated for βDF fission of ^{180}Tl and induced fission of the even-A isotopes ^{180,184,192,196,198}Hg. The asymmetric mass distribution of fission fragments of ^{180}Hg observed by Andreyev *et al.* (2010) is explained, and the mean kinetic energy is in good agreement with the experimental data. The change in the shape of the mass distribution from asymmetric to more symmetric is revealed with increasing A of the fissioning ^{A}Hg nucleus.

Panebianco *et al.* (2012) used the recently developed microscopic scission-point model, whereby the individual potential of each fragment is derived in the framework of Hartree-Fock-Bogoliubov (HFB) microscopic calculations with the Gogny effective nucleon-nucleon force, going far beyond the liquid drop description used in the original model by Wilkins. With this approach, the asymmetric fission mass distribution for the ^{180}Hg at low energy could be described on the sole basis of the fragment structure and deformed shell effects.

Thus, it appears that different theoretical approaches provide a robust description of the asymmetric mass split of ^{180}Hg. However, it is important to stress that quite different underlying mechanisms are proposed by different studies.

VII. FUTURE PROSPECTS IN βDF AND LOW-ENERGY FISSION STUDIES

To date, 26 βDF isotopes are known in three regions of the chart of nuclides; see Fig. 1: the neutron-rich Ac and Pa isotopes, and the neutron-deficient isotopes in the transuranium and lead regions. However, in many cases only scarce information is presently available. Substantial progress can be expected in all three regions, due to developments of new and/or improved production and detection methods. We highlight some of the interesting βDF studies feasible in the near future.

- In-depth βDF experiments: The main effort in all three βDF regions should concentrate on detailed experiments to reliably measure βDF probabilities, partial half-lives, and energy-mass distributions of fission fragments, similar to those performed, e.g., ^{180}Hg (Elseviers *et al.*, 2013). A direct measurement of the Z values is also needed to firmly establish the A and Z distributions of the fission fragments. The experiments with the laser-ionized isomerically pure beams of ^{192,194}At, ^{186,188}Bi, and ^{202}Fr should determine whether both isomers of each isotope undergo βDF and whether any difference exists in the βDF process of different isomers. The importance of these isotopes is further highlighted by the fact that their fissioning daughters (^{186,188}Pb, ^{192,194}Po, and ^{202}Rn) lie in the transitional region between ^{178,180}Hg, exhibiting asymmetric low-energy fission, and ^{204}Rn, which fissions symmetrically at similar excitation energies (Schmidt *et al.*, 2000); see Fig. 1. The first laser-assisted βDF studies of ^{194,196}At have already started at ISOLDE (Andreyev *et al.*, 2012).
- The search for new βDF cases: Dedicated searches for βDF of the neutron-rich ^{228,230,232}Fr and ^{228,230,232}Ac are possible at the ISOL facilities, such as, e.g., ISOLDE or Isotope Separator and Accelerator (ISAC) [TRIUMF (TRI-University Meson Facility)] (Bricault *et al.*, 1997). In contrast to the radiochemical studies of ^{228,230}Ac (Shuanggui *et al.*, 2001; Yanbing *et al.*, 2006), a unique Z and A identification of the parent isotope can be obtained in such experiments, along with the measurements of fission fragment energy and mass distributions. In earlier experiments in Gatchina (Mezilev *et al.*, 1990) only upper limits for βDF of ^{228,230,232}Fr and ^{232}Ac were obtained, being in the range of 10^{-7}–10^{-4}, which appear too high to expect the observation of βDF in these nuclei. Figure 14 shows the yields for the neutron-rich Fr isotopes measured at ISOLDE. With the reported beam intensities of $\sim 10^5$

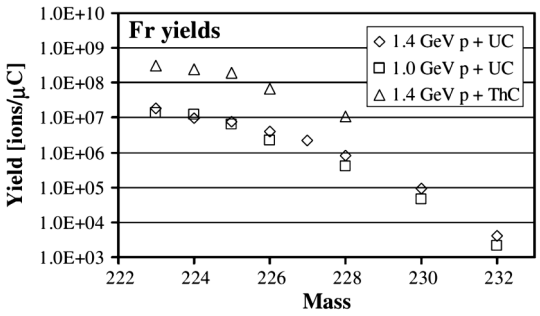

FIG. 14. Yields of neutron-rich francium isotopes measured at ISOLDE with uranium and thorium targets. From Peräjärvi *et al.*, 2004.

(^{230}Fr) and $\sim 5 \times 10^3$ (^{232}Fr), the βDF probabilities of $\sim 10^{-10}$–10^{-9} should be reachable. In the past, by using the multinucleon-transfer reactions of 11.4 MeV/u ^{238}U ions with ^{nat}W/Ta targets at the GSI ISOL mass separator (Gippert *et al.*, 1986), new isotopes ^{232}Ra and ^{233,234}Ac were produced. The use of this method to search for βDF of ^{232,234}Ac could be an interesting extension of the βDF studies of ^{230}Ac, also produced in the transfer reaction (Shuanggui *et al.*, 2001).

In the lead region, a search for βDF of the odd-A precursors should be performed, as for some of them the $Q_{EC} - B_f$ values can allow some feeding close to the top of the fission barrier; see, e.g., ^{193,195}At in Fig. 4. Finally, an important task is to move to the extremely neutron-deficient nuclides that have a dominant α-decay mode and very small β-branching ratios ($b_\beta < 1\%$). For such nuclei, due to the efficient detection of α decays and fission fragments, partial βDF half-lives can be determined without referring to the β decay. This can substantially increase the number of nuclides available for an analysis similar to that performed in Fig. 12.

The aforementioned goals require improved production and detection techniques. The more advanced in-flight recoil separators, such as S^3 [GANIL (Grand Accélérateur National d'Ions Lourds)] (Drouart *et al.*, 2011), will provide unprecedented opportunities to reach the neutron-deficient nuclei in the transuranium region, which is not accessible using the fragmentation-based ISOL techniques. Because of a substantial beam intensity increase, a gain by at least an order of magnitude in production rates can be expected. Combined with better separation capabilities and improved detection systems, this technique will certainly open a new era in βDF studies in the transuranium region. The same technique can also be used to study the shortest-lived βDF nuclides in the lead region, such as ^{192}At, which is not yet accessible to an ISOL facility due to its short half-life and a relatively long release time from the target-ion source.

Laser-based techniques, such as RILIS (Fedosseev *et al.*, 2012), Collinear Resonance Ionization Spectroscopy (CRIS) (Lynch *et al.*, 2012), and the recently developed IGLIS (Ferrer *et al.*, 2012), coupled to the S^3 separator, will further increase the sensitivity of the experiments and allow one to address the problem of the existence of two isomers in a βDF precursor.

More generally, as far as the low-energy fission studies are concerned, several promising projects are presently being developed. As a continuation of the Coulex-induced fission experiments with relativistic secondary beams (Schmidt, Benlliure, and Junghans, 2001), the next generation of such studies has recently been initiated by the SOFIA Collaboration at GSI. These experiments will benefit from the improved beam intensity of the initial ^{238}U beam and from detector developments which should enable the unique mass and charge identification of fission fragments with a precision of one unit.

In another recent approach, the Variable Mode Spectrometer (VAMOS) (GANIL) was used to study fission initiated by multinucleon transfer reactions in inverse kinematics between a ^{238}U beam and a ^{12}C target (Derkx *et al.*, 2010). The first experiments produced different minor actinides, within a range of excitation energies below 30 MeV.

A new ambitious method to study low-energy fission exploits the inelastic electron scattering off exotic radioactive beams in a colliding beam kinematics. Two such projects are currently underway: Electron Ion Scattering in a Storage Ring (ELISe) [FAIR (Facility for Antiproton and Ion Research)] (Simon, 2007) and Self-containing Radioactive Isotope Target (SCRIT) (RIKEN) (Suda *et al.*, 2009). Overall, substantial progress in βDF and low-energy fission studies is certainly expected in the near future.

ACKNOWLEDGMENTS

We thank S. Antalic, F. P. Heßberger, T. Ichikawa, A. Iwamoto, P. Möller, W. Nazarewicz, K. Nishio, J. Randrup, K.-H. Schmidt, A. J. Sierk, M. Veselský, and M. Warda for fruitful discussions. This work was supported by FWO-Vlaanderen (Belgium), by GOA/2010/010 (BOF KULeuven), by the IAP Belgian Science Policy (BriX network P7/12), by a grant from the European Research Council (ERC-2011-AdG-291561-HELIOS), by the United Kingdom Science and Technology Facilities Council (STFC), and by the Reimei Foundation of Advanced Science Research Center (ASRC) of JAEA (Japan).

REFERENCES

Andreev, A. V., G. G. Adamian, and N. V. Antonenko, 2012, Phys. Rev. C **86**, 044315.
Andreyev, A. N., D. D. Bogdanov, S. Saro, G. M. Ter-Akopian, M. Veselský, and A. V. Yeremin, 1993, Phys. Lett. B **312**, 49.
Andreyev, A. N., *et al.*, 2002, Eur. Phys. J. A **14**, 63.
Andreyev, A. N., *et al.*, 2005, Phys. Rev. C **72**, 014612.
Andreyev, A. N., *et al.*, 2006, Phys. Rev. C **73**, 024317.
Andreyev, A. N., *et al.*, 2009, Phys. Rev. C **79**, 064320.
Andreyev, A. N., *et al.*, 2010, Phys. Rev. Lett. **105**, 252502.
Andreyev, A. N., *et al.*, 2011, ISOLDE Proposal, http://cdsweb.cern.ch/record/1319032/files/INTC-P-235-ADD-2.pdf.
Andreyev, A. N., *et al.*, 2012, ISOLDE Proposal, http://cdsweb.cern.ch/record/1410652/files/INTC-P-319.pdf.
Andreyev, A. N., *et al.*, 2013, Phys. Rev. C **87**, 014317.
Antalic, S., *et al.*, 2010, Eur. Phys. J. A **43**, 35.
Armbruster, P., 1999, Rep. Prog. Phys. **62**, 465.
Audi, G., M. Wang, A. Wapstra, F. Kondev, M. MacCormick, X. Xu, and B. Pfeiffer, 2012, Chinese Phys. C **36**, 1287.

Baas-May, A., J. V. Kratz, and N. Trautmann, 1985, Z. Phys. A **322**, 457.
Balagna, J. P., G. P. Ford, D. C. Hoffman, and J. D. Knight, 1971, Phys. Rev. Lett. **26**, 145.
Batist, L. H., E. Y. Berlovich, V. V. Gavrilov, Y. N. Novikov, S. Y. Orlov, and V. I. Tikhonov, 1977, LNPI Report No. N363.
Berlovich, E. Y., and Y. N. Novikov, 1969, Phys. Lett. **29B**, 155.
Bricault, P. G., M. Dombsky, P. M. Schmor, and G. Stanford, 1997, Nucl. Instrum. Methods Phys. Res., Sect. B **126**, 231.
Csige, L., *et al.*, 2013, Phys. Rev. C **87**, 044321.
Davids, C. N., 2003, Nucl. Instrum. Methods Phys. Res., Sect. B **204**, 124.
Derkx, X., *et al.*, 2010, Eur. Phys. J. Web Conf. **2**, 07001.
Drouart, A., A. M. Amthor, D. Boutin, F. Déchery, J. A. Nolen, and H. Savajols, 2011, Eur. Phys. J. Web Conf. **17**, 14 004.
Elseviers, J., *et al.*, 2013, Phys. Rev. C (to be published).
ENSDF, 2013, Evaluated Nuclear Structure Data File, http://www.nndc.bnl.gov/ensdf/.
Escher, J. E., J. T. Burke, F. S. Dietrich, N. D. Scielzo, I. J. Thompson, and W. Younes, 2012, Rev. Mod. Phys. **84**, 353.
Fedosseev, V. N., *et al.*, 2012, Rev. Sci. Instrum. **83**, 02A903.
Ferrer, R., *et al.*, 2012, Nucl. Instrum. Methods Phys. Res., Sect. B **291**, 29.
Galeriu, U., 1983, J. Phys. G **9**, 309.
Gangrsky, Y. P., G. M. Marinesky, M. B. Miller, V. N. Samsuk, and I. F. Kharisov, 1978, Yad. Fiz. **27**, 894 [Sov. J. Nucl. Phys. **27**, 475 (1978)].
Gangrsky, Y. P., M. B. Miller, L. V. Mikhailov, and I. F. Kharisov, 1980, Yad. Fiz. **31**, 306 [Sov. J. Nucl. Phys. **31**, 162 (1980)].
Gippert, K. L., *et al.*, 1986, Nucl. Phys. A **453**, 1.
Habs, D., H. Klewe-Nebenius, V. Metag, B. Neumann, and H. J. Specht, 1978, Z. Phys. A **285**, 53.
Hahn, O., and F. Strassmann, 1939, Naturwissenschaften **27**, 11.
Hall, H., and D. C. Hoffman, 1992, Annu. Rev. Nucl. Part. Sci. **42**, 147.
Hall, H. L., K. E. Gregorich, R. A. Henderson, D. M. Lee, D. C. Hoffman, M. E. Bunker, M. M. Fowler, P. Lysaght, J. W. Starner, and J. B. Wilhelmy, 1989a, Phys. Rev. C **39**, 1866.
Hall, H. L., *et al.*, 1989b, Phys. Rev. Lett. **63**, 2548.
Hall, H. L., *et al.*, 1990a, Phys. Rev. C **42**, 1480.
Hall, H. L., *et al.*, 1990b, Phys. Rev. C **41**, 618.
Hingmann, R., W. Kuehn, V. Metag, R. Novotny, A. Ruckelshausen, H. Stroeher, F. P. Heßberger, S. Hofmann, G. Münzenberg, and W. Reisdorf, 1985, GSI Scientific Report No. 1984, p. 88.
Hoffman, D. C., 1989, Nucl. Phys. **A502**, 21.
Hoffman, D. C., *et al.*, 1990, Phys. Rev. C **41**, 631.
Hofmann, S., and G. Münzenberg, 2000, Rev. Mod. Phys. **72**, 733.
Ichikawa, T., A. Iwamoto, P. Möller, and A. J. Sierk, 2012, Phys. Rev. C **86**, 024610.
Izosimov, I., V. Kalinnikov, and A. Solnyshkin, 2011, Phys. Part. Nucl. **42**, 963.
Klapdor, H. V., C. O. Wene, I. N. Isosimov, and Y. W. Naumow, 1979, Z. Phys. A **292**, 249.
Kreek, S. A., *et al.*, 1994a, Phys. Rev. C **50**, 2288.
Kreek, S. A., *et al.*, 1994b, Phys. Rev. C **49**, 1859.
Kugler, E., 2000, Hyperfine Interact. **129**, 23.
Kuznetsov, V. I., and N. K. Skobelev, 1999, Phys. Part. Nucl. **30**, 666.
Kuznetsov, V. I., N. K. Skobelev, and G. N. Flerov, 1966, Yad. Fiz. **4**, 279 [Sov. J. Nucl. Phys. **4**, 202 (1967)].
Kuznetsov, V. I., N. K. Skobelev, and G. N. Flerov, 1967, Yad. Fiz. **5**, 271 [Sov. J. Nucl. Phys. **5**, 191 (1967)].
Lane, J. F. W., *et al.*, 2013, Phys. Rev. C **87**, 014318.
Lazarev, Y. A., Y. T. Oganessian, I. V. Shirokovsky, S. P. Tretyakova, V. K. Utyonkov, and G. V. Buklanov, 1987, Europhys. Lett. **4**, 893.
Lazarev, Y. A., Y. T. Oganessian, I. V. Shirokovsky, S. P. Tretyakova, V. K. Utyonkov, and G. V. Buklanov, 1992, Inst. Phys. Conf. Ser. **132**, 739.
Leino, M., 2003, Nucl. Instrum. Methods Phys. Res., Sect. B **204**, 129.
Liberati, V., *et al.*, 2013, unpublished.
Lynch, K. M., *et al.*, 2012, J. Phys. Conf. Ser. **381**, 012128.
Mamdouh, A., J. Pearson, M. Rayet, and F. Tondeur, 2001, Nucl. Phys. **A679**, 337.
Meyer, B. S., W. M. Howard, G. J. Mathews, K. Takahashi, P. Möller, and G. A. Leander, 1989, Phys. Rev. C **39**, 1876.
Mezilev, K. A., Y. N. Novikov, A. V. Popov, Y. Y. Sergeev, and V. I. Tikhonov, 1990, Z. Phys. A **337**, 109.
Möller, P., D. G. Madland, A. J. Sierk, and A. Iwamoto, 2001, Nature (London) **409**, 785.
Möller, P., J. R. Nix, W. D. Myers, and W. J. Swiatecki, 1995, At. Data Nucl. Data Tables **59**, 185.
Möller, P., J. Randrup, and A. Sierk, 2012, Phys. Rev. C **85**, 024306.
Möller, P., A. J. Sierk, T. Ichikawa, A. Iwamoto, R. Bengtsson, H. Uhrenholt, and S. Aberg, 2009, Phys. Rev. C **79**, 064304.
Münzenberg, G., W. Faust, S. Hofmann, K. Armbruster, P. Güttner, and H. Ewald, 1979, Nucl. Instrum. Methods **161**, 65.
Myers, W. D., and W. J. Świątecki, 1999, Phys. Rev. C **60**, 014606.
Ninov, V., F. Heßberger, S. Hofmann, H. Folger, G. Münzenberg, P. Armbruster, A. Yeremin, A. Popeko, M. Leino, and S. Saro, 1996, Z. Phys. A **356**, 11.
Panebianco, S., J.-L. Sida, H. Goutte, J.-F. Lemaître, N. Dubray, and S. Hilaire, 2012, Phys. Rev. C **86**, 064601.
Panov, I., E. Kolbe, B. Pfeiffer, T. Rauscher, K.-L. Kratz, and F.-K. Thielemann, 2005, Nucl. Phys. **A747**, 633.
Peräjärvi, K., J. Cerny, L. Fraile, A. Jokinen, A. Kankainen, U. Köster, and J. Äystö, 2004, Eur. Phys. J. A **21**, 7.
Petermann, I., K. Langanke, G. Martínez-Pinedo, I. Panov, P. G. Reinhard, and F. K. Thielemann, 2012, Eur. Phys. J. A **48**, 1.
Petrzhak, K. A., and G. N. Flerov, 1941, Usp. Fiz. Nauk **25**, 241 [Zh. Eksp. Teor. Fiz. **10**, 1013 (1940)].
Polikanov, S. M., V. Druin, V. Karnaukhov, V. Mikheev, A. Pleve, N. Skobelev, V. Subbotin, G. Ter-Akopyan, and V. Fomichev, 1962, Zh. Eksp. Teor. Fiz. **42**, 1464 [Sov. Phys. JETP **15**, 1062 (1962)].
Randrup, J., and P. Möller, 2011, Phys. Rev. Lett. **106**, 132503.
Rothe, S., *et al.*, 2013, Nat. Commun. **4**, 1835.
Schmidt, K.-H., J. Benlliure, and A. R. Junghans, 2001, Nucl. Phys. **A693**, 169.
Schmidt, K.-H., and B. Jurado, 2012, Phys. Procedia **31**, 147.
Schmidt, K.-H., *et al.*, 2000, Nucl. Phys. **A665**, 221.
Shaughnessy, D. A., K. E. Gregorich, M. R. Lane, C. A. Laue, D. M. Lee, C. A. McGrath, D. A. Strellis, E. R. Sylwester, P. A. Wilk, and D. C. Hoffman, 2001, Phys. Rev. C **63**, 037603.
Shaughnessy, D. A., *et al.*, 2000, Phys. Rev. C **61**, 044609.
Shaughnessy, D. A., *et al.*, 2002, Phys. Rev. C **65**, 024612.
Shuanggui, Y., Y. Weifan, X. Yanbing, P. Qiangyan, X. Bing, H. Jianjun, W. Dong, L. Yingjun, M. Taotao, and Y. Zhenguo, 2001, Eur. Phys. J. A **10**, 1.
Simon, H., 2007, Nucl. Phys. **A787**, 102.
Skobelev, N. K., 1972, Yad. Fiz. **15**, 444 [Sov. J. Nucl. Phys. **15**, 249 (1972)].
Staudt, A., M. Hirsch, K. Muto, and H. V. Klapdor-Kleingrothaus, 1990, Phys. Rev. Lett. **65**, 1543.

Suda, T., *et al.*, 2009, Phys. Rev. Lett. **102**, 102501.
Thielemann, F. K., J. Metzinger, and H. Klapdor, 1983, Z. Phys. A **309**, 301.
Veselský, M., A. N. Andreyev, S. Antalic, M. Huyse, P. Möller, K. Nishio, A. J. Sierk, P. Van Duppen, and M. Venhart, 2012, Phys. Rev. C **86**, 024308.
Wagemans, C., 1991, *The Nuclear Fission Process* (CRC Press, Boca Raton, FL).
Warda, M., A. Staszczak, and W. Nazarewicz, 2012, Phys. Rev. C **86**, 024601.
Wene, C. O., and S. A. E. Johansson, 1974, Phys. Scr. **10**, 156.
Wilkins, B. D., E. P. Steinberg, and R. R. Chasman, 1976, Phys. Rev. C **14**, 1832.
Yanbing, X., Z. Shengdong, D. Huajie, Y. Shuanggui, Y. Weifan, N. Yanning, L. Xiting, L. Yingjun, and X. Yonghou, 2006, Phys. Rev. C **74**, 047303.